AD-A047 511 NAVAL OCEAN RESEARCH AND DEVELOPMENT ACTIVITY NSTL S--ETC F/G 8/11
INTERPRETATION OF SINGLE-CHANNEL SEISMIC REFLECTION RECORDS,(U)
FEB 77 J A BALLARD

UNCLASSIFIED NORDA-1 NL

| OF |
AD
A047511

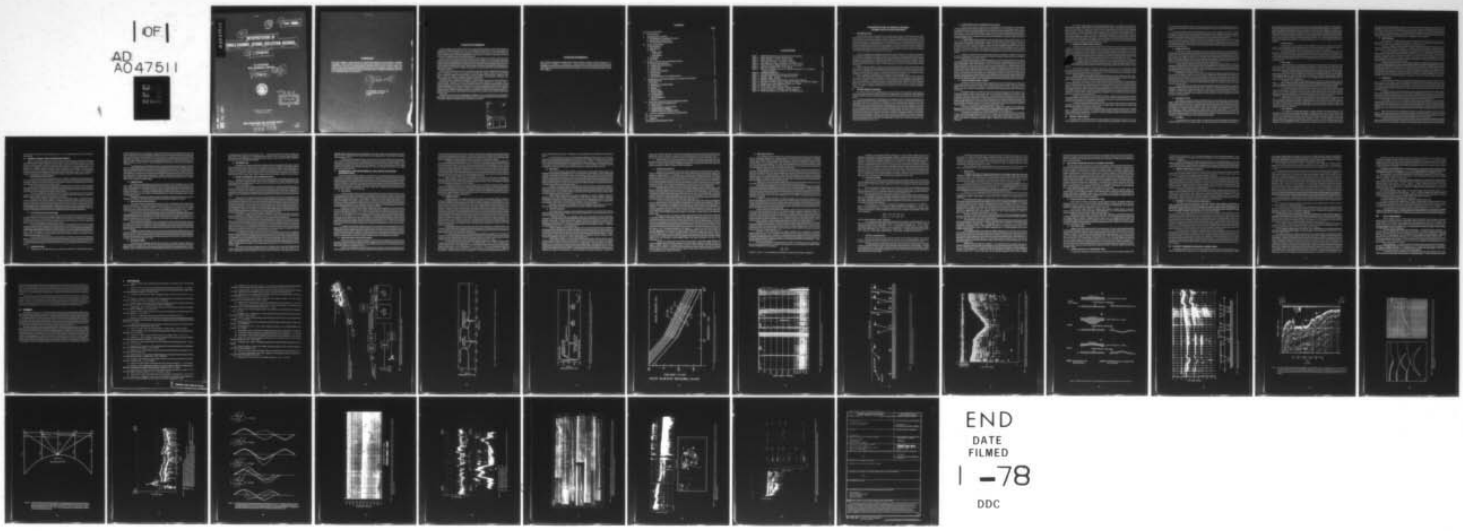

END
DATE
FILMED
1 -78
DDC

(12) (14) NORDA [redacted]-1

(6)

INTERPRETATION OF SINGLE-CHANNEL SEISMIC REFLECTION RECORDS

(10) J. ALAN BALLARD

SEA FLOOR DIVISION
NAVAL OCEANOGRAPHIC LABORATORY

(11) Feb[redacted] 1977 (12) 49 p.

NAVAL OCEAN RESEARCH AND DEVELOPMENT ACTIVITY
NSTL Station, Mississippi 39529

FOREWORD

This report is designed to assist beginning and experienced geoscientists in the techniques for quantitative interpretation of seismic reflection records. Most archival seismic reflection data were collected in the single-channel format. These data can provide background information required as input for acoustic models of the ocean floor and can lead to better specifications and solutions of many naval problems. A discussion of instrument theory and performance, as these factors influence record interpretation, is included for completeness. Comments on the usefulness of this report are welcomed.

C. G. DARRELL, CAPTAIN, USN
COMMANDING OFFICER
NORDA

EXECUTIVE SUMMARY

Normal incidence seismic reflection records are simply graphic presentations of travel times between an energy source, reflective interfaces, and one or more receivers. Interpretation of the data collected within this simple framework is complicated by the necessity for understanding the physics of the instrumentation, the environmental influences on the paths followed by the sound waves, or the effects of sediment sound velocity variation on the apparent shape of the reflective interfaces.

Sparkers, which create shock waves by vaporizing the salt water between two electrodes, and air guns which create shock waves by explosively emptying a high pressure air chamber, are the most widely used energy sources. Direct and reflected signals are received on linear arrays of piezoelectric crystal hydrophones which are configured to discriminate against horizontal and random near-field noises and amplify signals traveling at or near normal incidence to the plane of the receiver. Filters, amplifiers, and recorders also distort the incoming signals in a fashion similar to the environment. The effects of these factors must be understood before a meaningful analysis of the data can be made.

Vertical velocity variations are one of the more significant factors that must be considered before the apparent depth or time-section raw data can be converted to true depth data. Velocity variations may cause simple erosional channels to appear as structural features, or cause a significant reflecting horizon to appear to shoal, when, in reality, it is deepening. Calculating vertical velocity structure can be accomplished if drilling logs, wide-angle reflection data, or refraction data are available for a specific area.

Other factors which complicate the interpretation of normal incidence seismic records include diffraction or amplitude effects. A diffraction is the echo pattern produced by energy scattered from a sharp peak, edge, or similar irregularity, and can cause a fixed point reflector to appear to be a significant geologic structure or cause apparent displacement in the location of reflectors. Because the recording papers used for seismic reflection records have a finite dynamic range, the records have a qualitative amplitude component which is related to energy absorption, reflector thickness and roughness, and sediment physical properties through the reflection coefficients of successive layers. Both diffraction and amplitude effects are significant in quantitative interpretations of seismic data.

Despite all the environmental and interpretational constraints encountered during collection and evaluation of seismic data, this technique remains the most efficient method for developing reasonable and consistent quantitative geologic models of the sea floor and its covering layer of sediments.

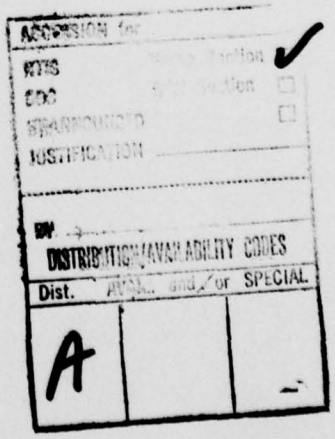

ACKNOWLEDGEMENTS

Joel S. Watkins (Geophysical Laboratory, Marine Science Institute, University of Texas at Galveston), G. E. Lawniczak, Jr., H. C. Eppert, Jr., J. E. Matthews, T. L. Holcombe, and R. S. Anderson (Naval Ocean Research and Development Activity) read and constructively edited versions of the manuscript. Special thanks are extended to Linda Thigpen for typing and editing the manuscript, relentlessly. The work was supported by DCNM (D) funding (DDF programs).

CONTENTS

ILLUSTRATIONS

INTERPRETATION OF SINGLE-CHANNEL SEISMIC REFLECTION RECORDS

I. INTRODUCTION

Normal incidence seismic reflection records are simply graphic displays of the total travel time of sound waves between a sound source, an impedance mismatch within the stratigraphic column, and a receiver. Before these records can be meaningfully related to variations in geological interfaces which they approximate, one must understand the behavior of acoustic energy, the equipment with which it is generated and received, and the environmental effects on the paths that it follows. The purpose of this report is to describe how the collection of single-channel seismic data may be fitted to a specific objective, and to define limits of accuracy and consistency of essentially qualitative data that are to be used quantitatively. Accordingly, both the basic principles involved, and the operational techniques employed for the two types of sound sources commonly used by oceanographic institutions to collect single-channel seismic data, are outlined.

In order to collect data more applicable to the solution of specific problems, it is important that equipment and technique be configured for the specific objective. For example, if the operational area consists of a thick section of uniform sediments, and the objective is to delineate the distribution of probable upper Tertiary reflectors, the equipment and technique used would be quite different from those with the goal of mapping "acoustic basement" topography beneath a variable thickness sediment cover. Other factors that should be evaluated before data collection begins is the amount of noise generated by the survey vessel, the towing operation, and the environment.

Once the data are collected, it is necessary to consider the distortions, to both the transmitted and the received signals, introduced by instrumentation before desired signals and other periodic events on the seismic record can be separated and the relationship between recorded signals and noises established. Also, compressional wave velocity variations, ray path and reflecting point variations, and amplitude variations contribute to the recording of data that are not true depictions of unique geologic events.

Once a reflected event representative of a geological variation is identified, the event must be positioned with respect to the geometries of the reflecting surfaces and the recording equipment. Errors inherent in conversion of analog data to a digital format with an X-Y coordinate digitizer are inconsequential with respect to the scale of most recordings. To establish consistency of scaled values, acoustic reflection horizons in the eastern North Atlantic serve to illustrate and define types of impedance mismatches which act as reflective surfaces. Figure 1 is a sketch of a typical single-channel seismic operation at sea and a block diagram of equipment commonly used.

II. SOUND ENERGY SOURCES

For more than half a century, geophysicists have worked to obtain continuous seismic representation of subsurface geology. Research to achieve this goal led to the development of nondestructive, rapidly repeatable acoustic sources for the seismic reflection profiling technique which has found great applicability in the deep ocean basins.

One of the first reported uses of a nondestructive or nonexplosive source to measure sediment thickness in water-covered areas was W. Smith's (1958) attempt to use a 12-kHz transducer to determine thicknesses and accumulation rates of recent sediments in Lake Mead. To improve instrumentation, MacClure et al. (1958) experimented with lower frequency transducers and developed the "Sonoprobe" which operated at 3.8 and 6.0 kHz. The lower frequencies and higher power thus obtained fostered several orders of magnitude improvement over previous efforts. Other nonexplosive source experiments were reported by Anderson (1953), who described the acoustic behavior of an electrical spark in seawater, and Padberg (1958), who pointed out the advantages of high-pressure air discharges as a seismic source. Other acoustic devices designed to operate in water-covered areas include propane/oxygen exploders, eddy-current transducers, displacement transducers, electrolysis generators, vacuum imploders, and explosively released steam. Despite these advances, the first successful marine reflection profiler used small blocks of fuse-detonated TNT fired at two- or three-minute intervals as an energy source (Ewing and Tirey, 1961).

A. CHARACTERISTICS OF A NONDESTRUCTIVE SOURCE

Sound sources must have certain common characteristics in order to qualify as a nondestructive, continually operating, marine seismic energy source. A source should have a broad frequency range in order to provide high frequencies for improved resolution and low frequencies for maximum penetration. Other characteristics include: (1) very short time period between initiation of the source discharge and maximum power output of the initial pulse in order to obtain maximum power transfer to the water column, and higher frequencies resulting in improved resolution; and (2) no bubble pulse associated with initial discharge in order to give a single output and an unequivocal reflected signal.

To make shipboard operations feasible, a source must be sturdy enough to be towed at 18.5 km/hr (10 kts) or more; flexible enough to be discharged as slow as once per minute, or fast as once per second; and mechanically and electrically simple enough to achieve low initial cost, operational reliability, and ease of maintenance by relatively inexperienced people. In addition, shipboard feasibility is enhanced if the source does not require extensive pre-installation modifications to the ship and is sufficiently lightweight so that it may be launched or recovered under rigorous sea conditions without danger to the few people usually available for handling assistance. Finally, a source is not acceptable if it is destructive to marine life or if it produces offensive by-products.

Obviously, no particular sound source is uniquely suited for all applications. Therefore, the assembler of a seismic profiling system must make value judgments based on his particular application and his evaluation of the limiting characteristics of an acoustic source.

Because the sparker source is relatively inexpensive to buy and install, easily towed and handled at sea, reliable and easily maintained by frequently inexperienced technicians, and nondestructive to marine life, the Naval Oceanographic Office, (NAVOCEANO), as well as many other institutions and agencies with marine geophysics programs, initially chose the sparker as their basic sound energy source. In reaching this decision, the sparker's bubble pulse was perceived as unavoidable, if not helpful, and its deficiency in the low-frequency portion of the spectrum was considered inconsequential because attenuation through the water column is not a serious problem. Ocean-bottom sedimentary layers are frequently thin and respond well to higher frequency sound waves. Later improvements in technology led many oceanographic institutions to adopt air gun energy sources because of their higher power and lower frequency output. Because most of the archived, single-channel seismic data were collected with either sparker or air gun energy sources, these sources will be examined to show the characteristics of the signals they produce and the interpretational constraints that these signals impose on the record.

B. SPARKER SEISMIC ENERGY SOURCE

Sparkers work because electrical energy storage devices will almost instantaneously (on the order of microseconds) release most of their energy, which required several seconds to develop. When the electrodes, between which the energy flows, are immersed in a conducting fluid such as salt water, the energy may be of sufficient intensity to vaporize the fluid between the electrodes, thereby creating a high-intensity, short duration, shock wave.

According to Kramer et al. (1969), the arcing of current from one electrode to another creates a hot and incandescent plasma of steam, ionized copper "gas", and free electrons. Expansion of this "steam" vapor produces the initial shock wave at seismic frequencies. The energy output of the initial pulse is primarily a function of capacitor bank storage voltage because stored energy varies as the square of the voltage, but only as the first power of the capacitance (Knott, 1970). As a result, Knott believes that it is important to operate the sparker at the highest possible voltage levels in order to obtain both a high-peak/pressure pulse and a long-period bubble pulse since the length of the bubble pulse period is indicative of energy output. If a high-frequency pulse is required to improve resolution, it may be obtained by reducing capacitance (Knott, 1970).

The size and shape of the initial discharge pulse is related to the number, size, and spacing of electrodes, and to other rather ill-defined parameters such as water temperature, salinity, and electrode tow depth. These factors are, of course, in addition to the electrical characteristics of the storage units.

In the sparker arrangement used on NAVOCEANO ships, the 30-kJ capacitor banks are charged at 14,500v and then discharged between two 6mm (¼ in.) copper wires encased, except for tips, in nylon insulation and rigidly separated by a 0.5m spacer. Because only the tips of the electrodes are exposed to salt water, a point-source is effectively produced. Figure 2 illustrates the signal waveform typical of this installation.

The "steam" bubble produced by the initial discharge expands to its maximum volume within a few milliseconds and then rapidly collapses. The collapse of the bubble and the rush of water into the created cavity generate a second wave, or "bubble" pulse, which contains an appreciable portion of the total power available from the sparker. The bubble created by the sparker is unique in that it is created primarily by steam. When the steam condenses on the first oscillations, further oscillations of the bubble pulse are prevented (Figure 2). According to Kramer et al. (1969), 25 msec is an average bubble-pulse period for a 30-kJ sparker, but other records show bubble pulses with periods of about 13 msec (Figure 2). The approximate peak frequency spectrum of the bubble pulse is the reciprocal of the period, and will vary between 30 and 80 Hz for most of the systems commonly used. The oscillation of the bubble pulse can be used to increase the energy radiated at lower frequencies, and thus enhance penetration (Kramer et al., 1969).

C. PNEUMATIC SEISMIC ENERGY SOURCE

Despite increases in power output achieved by the use of larger, more powerful capacitors, the sparker remains a very inefficient method for generating seismic energy. To increase the total power output and increase penetration by lowering the frequency spectrum, most oceanographic institutions have added air guns to their inventory of seismic energy sources. Although the costs, operational simplicity, and reliability of air guns and sparkers are comparable, the increase in power and decrease in frequency are paid for by a decrease in resolution caused by the paucity of higher frequencies and the multiplicity of oscillations of the bubble pulse. This latter factor is readily evident in Figure 3, which shows the waveform of a 225-in^3 air gun (Mero and Freitag, 1974).

Air guns produce shock waves because high-pressure air, normally at 2,000 psi, can be explosively released from its storage chamber. This suddenly released air creates a spherical bubble whose pressure is momentarily in excess of ambient hydrostatic pressure and generates acoustic energy by displacing a quantity of water. The air bubble oscillates several times (Figure 3) while rising through the water column and eventually vents to the surface.

Air gun frequency output is a function of air pressure, chamber size, and gun depth (Giles, 1968). Increasing the size of the air chamber has the same effect as increasing the pressure, i.e., it increases the size of the bubble and decreases the frequency. Conversely, an increase in tow depth increases the hydrostatic pressure on the air bubble and results in an increase in frequency.

Greatly increased power outputs may be routinely obtained from air guns relative to sparkers. Calculations show that a 300in^3 air gun (probably the most common size) is approximately equivalent to a 450,000-J sparker, about three times the size of the largest sparker system presently operating.

Air guns can be grouped in an array of various chamber sizes to greatly enhance the output signal and diminish bubble pulses. Use of multiple air gun arrays requires that several air compressors be installed aboard ship. The resulting expense and inordinate amount of ship space required for several air compressors make this means of improving the output signal somewhat less cost effective for institutions conducting multi-faceted oceanographic operations. Other available air gun bubble suppression devices include a wave shaper, which is an air chamber insert with a hole cut in the top so that part of the high-pressure air is released explosively, and part is released more slowly in order to counteract bubble pulse development. The device is effective, but requires about twice the air capacity for a given chamber size.

Because of their high power and low frequency spectrum, air guns are used almost exclusively for wide-angle reflection and refraction surveys in the deep ocean. Data collected by these techniques are used to calculate interval velocities and velocity gradients within the sediment column in order that travel times to reflecting horizons can be converted to true depths to these interfaces.

In addition, the signal shape generated by an air gun is extremely repetitive relative to the signal shape generated by a sparker discharge. As a result, the air gun output signal is more amenable to digital signal processing techniques than is a sparker's output signal.

Because of the relatively long time interval between the direct pulse and the oscillations of the bubble pulse — usually more than 100 msec — it is possible to resolve reflectors between these two events, assuming that the bubble pulse is identified and neutralized. If the data are digitally processed, the bubble pulse may be removed by deconvolution techniques.

III. SIGNAL PROCESSING

There may well be a millionfold variation in seismic energies from the initial source output to the weakest returning reflection. As a result, some form of on-line signal processing is required before a seismic cross-section

can be printed and evaluated. In addition to removing many spurious signals and thus simplifying interpretations, the signal processing equipment also introduces signal distortions that may complicate interpretations for the unwary.

The basic data collection and processing elements for routine, on-line operations most commonly include hydrophones connected as arrays to receive echoes, preamplifiers to boost signals from the towed hydrophone array, filters to emphasize signals in those frequency ranges containing the most pertinent information, amplifiers to boost filtered signals to printing levels, and facsimile or line scan recorders to display the data.

In recent years, many technological advances have substituted digital computers for these analog approaches to signal processing. However, for routine reconnaissance operations at sea, and as a real-time monitor for digital or multi-channel records, data are normally recorded in an analog format. If an area is selected for a detailed investigation, then seismic data may be recorded on magnetic tape and subjected to the appropriate digital processing techniques.

A. SIGNAL DETECTION

A hydrophone is a geophone suitable for use at sea. Geophones operate on either electrodynamic, variable reluctance, or piezoelectric principles. Because electrodynamic-type geophones attempt to measure the displacement of the earth which is generated by seismic waves, and thus require a simulated separation from the earth, they are not suitable for use at sea. On the other hand, variable reluctance and piezoelectric-type geophones are planted within the medium and are capable of sensing pressure variations. Because pressure is equal to (mass times acceleration)/area, and both mass and area are fixed, measured pressure variations are proportional to acceleration which is the second-time derivative of displacement.

Variable reluctance geophones generate electrical signals when pressure changes on soft iron diaphragms on opposite sides of the geophone cause the diaphragms to move and thus vary the magnetic reluctance. Reluctance is the magnetic analog of resistance in electrical circuits. Variable reluctance hydrophones are capable of measuring pressure variations, but for a given hydrostatic pressure, the power output increases with increasing frequency (Evenden and Stone, 1971).

Piezoelectricity is a property of certain crystals that cause them to develop an electrical potential when they are deformed. Because certain manufactured materials, notably barium titanite, possess this property and may be cast in any desired shape or size, they are used almost exclusively in marine hydrophones. Piezoelectric hydrophones produce a voltage output which is proportional to instantaneous water pressure and uniform for a broad range of frequencies. The major disadvantage in piezoelectric hydrophones is that their output impedance is very high so that a transformer is required to match impedances between the hydrophone and the preamplifier (Evenden and Stone, 1971).

The big problem with both variable reluctance and piezoelectric hydrophones is that they are unable to discriminate against pressure variation from any source or direction. To reduce this problem, hydrophones are connected in parallel and/or series-wired linear arrays, and encased in plastic tubing filled with castor oil, kerosene, or a similar buoyant dielectric. The dielectric increases hydrophone coupling and decreases salt-water corrosion; buoyance makes depth control possible by selective weighing. The value of hydrophone arrays are discussed in a following section.

B. PREAMPLIFICATION

Preamplifiers are required to supply the additional power that weak signals need to overcome cable losses, to match impedances between the hydrophone array and the cable, and to help suppress the very strong signals radiating directly from the source. These seemingly contradictory requirements are met because seismic preamplifiers require a very high input impedance to match the high impedance of low-frequency hydrophones. For example, the Teledyne Exploration Company's Model 24257 hydrophone array preamplifier has a 510-kΩ input impedance. In addition, preamplifiers are usually relatively low-gain (20dB) devices. This combination permits preamplifiers to maximize the weakest signals which are frequently those with the lowest frequency, and minimize the strongest signals if they contain appreciably higher frequency components, because the high input impedance increases the hydrophone array's signal damping capability.

C. FILTERING

An electrical filter, as the name implies, is an electronic device which attenuates those signals with frequencies higher or lower than a selected value, and limits recorded data to those ranges that emphasize a

particular feature. In this manner, the filter may aid resolution by enhancing higher frequencies, increase penetration by reducing higher frequencies and allowing more gain to be added to the lower frequencies, or by discriminating against cable or array vibrations. Filters are categorized in a variety of fashions depending on whether or not power is required for operation (active or passive), or on which side of their cut-off frequency the passband lies (high-pass or low-pass); or if high-pass, whether or not the inductor has a capacitor in series (with series capacitor, m-derived; or without, constant K); or if low-pass, whether or not the inductor has a capacitor in parallel (with capacitor in parallel, m-derived; or without, constant K) (Evenden and Stone, 1971). Seismic systems usually have a filter inserted between the preamplifier and the primary amplifier (Figure 1), or built as an integral part of the primary amplifier.

1. Passive Filters

Passive filters require no power for their operation, but suffer from relatively high insertion losses — differences between input and output levels. For this reason, and because of the size and expense of laminated iron core inductors, passive filters are not widely used in marine seismic equipment.

In practical applications, the m-derived passive filter has a very steep slope (greater than 20 dB/octave), but poor impulse response; while the constant-K passive filter has a more gentle slope (greater than 12 dB octave), but has a much better impulse response. As a result, the m-derived filter is more frequently used with amplifiers connected to digital recorders because impulse response is not as important in digital processing as in analog processing (Evenden and Stone, 1971). The constant-K filter seems more suited for amplifiers driving analog recorders.

2. Active Filters

When a passive filter is energized with a single impulse, which is always made up of equal amounts of all frequencies, the filter responds by attenuating some frequencies and shifting the phases of others (M. Smith, 1958). As a result, a single-impulse input emerges from the filter as a two or more cycle wave train. This phenomenon leads to the concept of differentiating and integrating circuits which make active filtering possible.

If the series resistor and capacitor in an RC filter are small enough to make $\omega RC \approx 0$ over a specified frequency range, then the output voltage from the circuit is the "equivalent of passing it through a system whose amplitude-frequency response is directly proportional to frequency, and whose phase-frequency response is a constant 90° lead" (Evenden and Stone, 1971, p. 35). This output response, when measured across the resistor, is commonly referred to as differentiation.

Conversely, if the resistance and capacitance in the RC filter are made very large such that $\omega RC \approx \infty$, then the voltage across the capacitor "has an amplitude-frequency response which is inversely proportional to frequency, and a phase-frequency response which is a constant 90° lag" (Evenden and Stone, 1971, p. 36). This type circuit response, when measured across the capacitor, is commonly called integration.

A waveform passed through a differentiating circuit emerges as a series of spikes, while the same waveform passed through an integrating circuit emerges as a broad curve. When a differentiator and an integrator operate on the waveform sequentially, a frequency band is defined. Better frequency discrimination and less distortion are achieved by feeding as much as possible of the filtered signal back through an amplifier capable of responding to frequencies all the way down to dc. This feedback process defines an active filter.

Active filters with steep slopes and sharp frequency cutoffs may be obtained by operating several such combinations in tandem. For example, Teledyne Exploration model 25950 seismic amplifier uses three cascaded stages of active filtering between the preamplifier and the primary amplifier in order to obtain maximum filter slopes of 36 dB/octave. The availability, compactness, and low cost of reliable transistors, resistors, and capacitors combined with easily achievable amplifier stability make active filtering one of the most widely used analog signal processing techniques.

3. Filter Selection

The tradeoff in filter bandwidth selection is between resolution and noise interference. If the bandwidth is set too wide, the multiplicity of wavelengths of returning signals will constructively and destructively interfere, thus creating signals of different wavelengths and amplitudes that produce a spurious clutter on the record. On the other hand, if the bandwidth is set too narrow, then certain combinations of reflector spacing may well eliminate significant returns and create false "transparent" zones. The center frequency of a particular bandpass is the square root of the product of the end points. For example, a 20- to 125-Hz bandpass has a center frequency of 50 Hz, $(\sqrt{(20)(125)})$. The filtered range should be at least an octave wide—the higher cutoff frequency

twice that of the lower cutoff frequency. Selection of a filter with a very steep low-frequency cutoff slope (24 to 36 dB/octave) helps to remove lower frequency tow noises. The upper frequency cutoff seems to be less critical. If 60-Hz pickup from the ship's electrical system proves troublesome, a notch filter, which severely attenuates signal over a very narrow frequency range, may be used without disturbing the other frequency components. Filters always attenuate some of the signal levels within the bandpass. This insertion loss is frequency-related such that changes in filter bandpass will necessitate changes in amplification in linear amplifiers.

D. AMPLIFICATION

The amplitude of the filtered signal is frequently below the threshold printing level of the facsimile or tape recorder being used. To multiply signal voltages to acceptable levels, a high-gain, low-noise amplifier is inserted into the seismic system between the filters and the recorders (Figure 1).

There are a multitude of seismic amplifier designs, but all have several common characteristics. For example, input impedance is always much lower (10^{3} times) than is true for preamplifiers, and output impedance is even lower (10^{5} times) than the input impedance. Low impedances retard transient 60-Hz electrical pickup.

Many seismic amplifiers can accept signals ranging from 0.3 to 10^{-7}V, and deliver an 0.6V signal after several stages of amplification. Stable low frequency amplification is considered more difficult to obtain than high frequency amplification because capacitive reactance, the capacitor's resistance analog, increases with decreasing frequency. When it is necessary to cascade several stages of transistorized amplifiers to achieve adequate signal gain, the gain in the low frequency portion of the spectrum is controlled primarily by the reactance of the interstage coupling capacitors (Brophy, 1966).

Among the several schemes for seismic signal amplification, the differential input amplifier is widely used because its amplification factor can be easily controlled by varying the resistance ratio between the two input terminals. The voltage difference between the two input terminals is the signal that is amplified. Other amplifiers are designed to increase the amplifier gain as the signal level decreases. If the gain of each amplifier is automatically adjusted as the signal level varies, then the amplifier is designated automatic gain controlled (AGC). On the other hand, if the amplifier gain is buffered in pre-determined steps to a pre-determined level, then the amplifier is designated programmed gain controlled (PGC). Both AGC and PGC are commonly supplied options on seismic amplifiers, however, if true amplitude information is required from the data, then PGC recording is necessary.

E. RECORDING

With the exception of limited areas surveyed with closely spaced grids, structures in the ocean are so poorly known that most seismic lines are essentially reconnaissance lines. When sufficient data have been accumulated to permit the geophysicist to precisely define his requirements, then it may be practical to record data in the more easily processed digital format. However, given the current constraints under which most oceanographic vessels operate, the graphic record made on board ship is likely to remain the primary seismic data presentation format.

Facsimile or line scan recorders work because the recording paper conducts electricity. When an electrical current is applied to the styli carrier bar, the stylus burns the paper wherever the stylus is in contact with the paper at the instant of energizing. Recorders are constructed so that only one stylus touches the paper at any one time. Electronic circuitry necessary to discharge the sound source is usually energized by initial contact between the stylus and the paper, thus, the recorder provides the timing control for the seismic system.

The number of lines per inch of recording controls the ease and reliability of visual correlation. NAVOCEANO uses 150 lines per inch for its master record because the slight overlap of individual line scans produces greater data density and enhances the correlation of subtle differences. The slave recorder is frequently adjusted to 50, 75, or 100 lines per inch, depending on model of recorder and geologic feature being studied. Experience has shown that a slight gray background highlights weaker reflections without detracting from stronger events.

Both wet and dry types of recording papers are widely used. Wet paper probably has a somewhat wide dynamic range, but tends to wrinkle and distort with changes in humidity. Dry paper is immune to humidity changes, but smudges badly and has a print odor that may be offensive in confined quarters aboard ship. Up to 23 dB dynamic range is possible with most of the recording papers now in use. (Knott, 1970).

If any secondary data processing is likely to be required, seismic data should be recorded on magnetic tape. Analog recorders have dynamic ranges more than twice the dynamic range of the best variable density recorder. One of the chief advantages of magnetically recorded data is that selected areas can be reprocessed

and presented at a horizontal to vertical scale ratio of 1:1. Such a presentation adds an extra dimension to interpretations.

IV. SIGNALS, NOISES, AND HYDROPHONE ARRAYS

When a sound wave travels through the ocean, the water is alternately squeezed together (compressed) and stretched apart (rarefied). Because of this phenomenon, devices (geophones) capable of converting mechanical energy (pressure) to electrical signals are used to detect both the intensity and frequency of the passing wave. A hydrophone, however, has two shortcomings. Because it is a pressure-sensitive device, it will respond to any change in pressure, regardless of origin; and because the wavelength of energy at seismic frequencies is very long compared to a practical size for hydrophones (30m vs. 0.03m), the hydrophone is inherently unable to discriminate against pressure differentials from any direction (Albers, 1965). To reduce the impact of these problems, hydrophones are connected in various configurations called arrays or streamers.

A. NOISE SOURCES AND CONTROL

As a sound wave travels outward from its source, its intensity is diminished by spreading of the wave front and absorption by the medium through which it is traveling. Eventually, signal levels decay to an intensity that is less than, or equal to, the environmental noise in which the system is operating, and desirable signals (reflections from subsurface acoustic horizons) are obscured by noise.

Noise, commonly defined as unwanted signal, is actually made up of random and coherent components. Random noise is locally generated, statistically uncorrelated energy, while coherent noise is statistically correlated and behaves in much the same fashion as desirable signal energy. For maximum inhibitory effectiveness, the two must be distinguished and treated in different fashions.

The sum of reverberation and field noises which cannot be rejected establishes the minimum signal level that can be recorded; thus, the incoming signal must exceed these noise levels. The greater the difference between these two values, the greater the resolution of the recording.

Significant noise generators capable of obscuring incoming signals include: (1) propeller cavitation, shipboard machinery noises, and ship vibrations; (2) turbulence created by an object being towed through the water; (3) ambient noise created by the prevailing sea state and local faunal sounds; (4) cable strumming and hydrophone acceleration caused by the stress of towing and wave motion; (5) electrical noise caused by the ship's 60-Hz operating power and crosstalk between various electrical conductors; and (6) reverberations. Other undesirable effects such as multiples, diffractions, and bubble pulses are often recorded, but these are functions of the source or the geological environment and will be discussed along with structural interpretations.

B. CAVITATION AND OTHER SHIP NOISE

Local hydrostatic pressures may be reduced to less than the ambient vapor pressure of water by extreme agitation, such as that due to propeller blades driving into the water, creating bubbles. When these bubbles move into areas of higher pressure and oscillate, noise is emitted just as in bubble pulse oscillations associated with seismic sources. This noise is called cavitation, and serves not only as a source of undesirable signal, but also as a baffle capable of screening seismic returns.

Mechanical vibrations produced by operating machinery directly coupled to the ship's hull are capable of producing noise at seismic frequencies. The relative intensities of mechanically coupled and cavitation noises are functions of ship's speed and displacement. At slow speeds (15 km/hr), the mechanical noises predominate, while at higher speeds (greater than 22 km/hr), cavitation becomes most important (National Defense Research Comm., 1946). Low-frequency (30-40 Hz) rhythmic noise frequently seen on seismic records, particularly in shallow water, is very likely due to mechanically coupled engine vibrations rather than to propeller noise as suggested by Bedenbender et al. (1970).

The sound field radiated by the ship and its equipment is omnidirectional. As a result, the deleterious effects of this noise source may be reduced by increasing the tow distance, by virtue of the receiving directionality of the hydrophone array, and by raising the low-frequency filter cutoff. As in the case of ambient noise, ship's noise is inversely proportional to frequency at the rate of about 7 dB per octave (National Defense Research Comm., 1946).

C. TURBULENT NOISE

Turbulent noise, also called flow noise, is created by movement of an object through the water.

Pressure distribution around a moving object is usually high at the leading edge; very low along the top, sides, and bottom surfaces; and high at the trailing edge. If the object is blunt, then the distance between the high-pressure zones and low-pressure zones becomes very short, the pressure rises rapidly, the boundary layer becomes separated from the object, and the pressure zones coalesce to form a broad, eddying wake downstream of the object. The effect of turbulent noise can be quite substantial; Bedenbender et al. (1970) report sound pressure spectrum levels in excess of 10 dB re 1 mbar for frequencies less than 80 Hz when the array's low speed is 18.5 km/hr.

The turbulent effect is magnified if the surface of the towed object is rough and the speed is relatively high. For example, Bedenbender et al. (1970) have heuristically determined that surface roughness becomes significant in producing noise when the height of the surface irregularity exceeds 0.06 in. (0.15 cm) divided by the ship's speed in knots. Thus, at 18.5 km/hr (10 kts), an irregularity greater than 0.0152 cm (0.006 in.) will cause some turbulence. In practical terms, this means that the hydrophone array should be kept clear of the wake of the ship, sound source, or even the towed magnetometer. In addition, extraneous chafing gear, tape, hose clamps, ballast weights, etc., should be removed or streamlined. Also it may be necessary to add fairing to the streamer cable to reduce formation of turbulent eddies.

D. AMBIENT NOISE

Sea surface noise generated by wind stress is the dominant source of ambient noise in the open ocean. Figure 4 shows the relationship between wave height, frequency, and sound pressure spectrum level (Urick, 1967): Mean pressure calculations, based on Figure 4, show that ambient wave noise decreases by an order of magnitude for 1-, 5-, and 8-foot wave heights, when the frequency is raised from 10 Hz to 50 Hz. The frequency-noise levels for 1- to 8-foot wave heights decrease by a factor of about 3 when the frequency is raised from 50 Hz to 100 Hz. Thus, close attention to low-pass filtering and sea state can drastically reduce noise and increase signal resolution.

Raindrops, marine life, and passing ship traffic all contribute to the level or ambient noise at seismic frequencies in the ocean. These effects are all transitory and can seldom be predicted or avoided.

E. VIBRATION AND ACCELLERATION

One need only stand on the afterdeck and watch the motions of a hydrophone array to appreciate the fact that considerable noise is generated by constantly varying tow tension. The pitch, roll, and yaw of the ship all produce static and dynamic pressure variations as well as accelerations in the towed array. At seismic frequencies, noises created by accelerations are an order of magnitude more significant than noises created by other motions and may reach maximum amplitudes of as much as 24 dB (Bedenbender et al., 1970).

On the other hand, Schoenberger and Mifsud (1974b) have shown that in relatively calm seas and at towing speeds above 10 km/hr that cable noise far outstrips electrical and ambient noises as the major source of undesirable signal. Rather than cable strumming, however, these authors believe that pressure fluctuations due to water flow (turbulence) cause much of this noise. Further, these noises occur between 10 and 25 Hz and are difficult to remove by low-frequency filtering.

Most hydrophone arrays include a stretch or compliant section to reduce the effects of cable strumming and vibration. If this proves to be inadequate in a particular installation, some gain may be realized by towing the array with elastic or nylon line which will serve to further insulate the array from erratic ship motions which induce strumming and accelerations. In addition, the cable fairing recommended to reduce turbulent noise should help reduce strumming.

In addition to producing ambient noise, wave motion (sea state) produces accelerations which can be quite large. Acceleration noises are controlled by mounting crystal hydrophone elements symmetrically about their sensitive axes, thus, a position change is recorded as both positive and negative pressures of equal amplitudes. The sum of these pressures is zero. Acceleration cancellation techniques can provide up to 12 dB improvement in the signal/noise ratio (Luehrmann et al., 1970).

F. ELECTRICAL NOISE

In permanent ship installations, electrical noises are usually not a significant problem. However, on ships-of-opportunity, transient 60-Hz noise from the ship's operating equipment may intrude into the seismic passband. Thus, it is imperative that all of the seismic equipment be carefully and thoroughly grounded. Even this precaution might not prevent noise override from high-powered transmitters such as the ship's radio. Such noise

can be disastrous to the seismic record (Figure 5). Low ($\approx$ 10Ω) output impedance of the seismic amplifiers will help minimize 60-Hz electrical noise. High-voltage seismic sources, such as a sparker, frequently produce transient spikes on simultaneously recorded data. Physical separation of the sensors and cables or addition of blanking circuits may help alleviate this problem.

G. REVERBERATION

Reverberation is energy scattered back toward the source by irregularities in the medium, and, as such, represents an entirely different class of noise. Reverberation has a practically unpredictable amplitude because the location and the magnitude of the irregularities are continually changing. Volume reverberation is reverberation from the water column caused by air bubbles, suspended solids, marine life, and local fluctuations of sound velocity resulting from random temperature and density variations. Bottom reverberation is a function of bottom sediment size and type, bottom slope or irregularity, area of insonification, frequency, and pulse length.

H. SIGNAL ENHANCEMENT AND HYDROPHONE ARRAYS

The goal of maximizing the signal/noise ratio has been attacked by using multiple groupings of hydrophones in series and/or parallel connection. Linear arrays of hydrophones may achieve directionality because arrays behave as an extended receiver or antenna. In this case, the array is much more sensitive in the plane perpendicular to its linear dimension.

Linear array design is based on the following assumptions: the desired signal originates from a distance sufficiently great so that the signal arrives at the hydrophone array as a plane wave, the incoming signal is in the plane of maximum array sensitivity, and the noise is predominantly local. Within these constraints, the hydrophones are then spaced far enough apart so that the locally generated noises arrive at each hydrophone at a different time and are statistically uncorrelated, while distant signals arrive simultaneously and are summed by the array.

Improvement in the signal/noise ratio can be approximated from the number of hydrophones in the array if the noise sources are all random. This improvement occurs because the random noise energy received by each hydrophone is distributed in a normal curve with a standard deviation related to the square root of the number of samples of noise energy. As a result, the total noise energy output of the hydrophone array is the product of the number of hydrophones (n) and the square root of the random noise output of each hydrophone in the array ($n^{1/2}$) (Schoenberger and Mifsud, 1974b). Because the signals are identical and in phase, the signal energy output by each hydrophone in the array is not random. Thus, the total signal energy output of the hydrophone array is the product of (n) identical signals from (n) hydrophones. Therefore, the near field, random, signal/noise improvement is approximately equal to ($n^{1/2}$), where (n) is the number of hydrophones in the array.

If the noise is coherent, individual hydrophone elements in the array cannot distinguish noises from signals. Nevertheless, the hydrophones coupled as an array can provide some signal/noise improvement because the array acts as an extended receiver having zones of greater and lesser sensitivities.

The zone of maximum sensitivity (main lobe) is perpendicular to the long axis of the array such that any coherent noise originating outside the main lobe is received with reduced amplitude. The width of the main lobe (directionality of the array) decreases with increasing length of the array and increasing frequency of the received signal (Luehrmann et al., 1970). Simply adding hydrophones to increase the length of the array and increasing the frequency will not solve all the noise problems. In the first case, the array cannot resolve features smaller in lateral extent than the length of the array; and, in the second case, increasing the frequency increases both bottom reverberations and attenuation losses in the bottom (Luehrmann et al., 1970).

The magnitude of the signal/noise increase due to the directionality of the array can be estimated, because the main receiving lobe is perpendicular to the long axis of the array and passes through the midpoint of the array. Therefore, the array's total signal power gain ($G^2\theta$) can be taken to have the value (n^2) everywhere inside the beamwidth (λ/D) and zero outside the beamwidth. The array's total noise power gain is ($\lambda/2D[n^2]$), because of the lack of correlation between the distant noise sources (bottom reverberation, side echoes, etc.) (Horton, 1969). Therefore, the signal/noise improvement factor is ($2D/\lambda$) for the distant noise background when (D) is the length of a hydrophone array made up of (n) equally spaced hydrophones and (λ) is the wavelength of sound (Horton, 1969).

In the case of the Teledyne Exploration Model 24257 hydrophone array, widely used for single-channel marine seismic work, 25 groups of two hydrophones each are spaced about 46 cm (18 in.) apart to form an 11m array. A second identical array is attached to form a total of 22m of active section. The output signal from each

hydrophone pair is alternatively fed into two preamplifiers. This electronic interlacing minimizes random noise by a factor of 10 ($100^{1/2}$). The coherent noise reduction factor ($2D/\lambda$) is approximately 1.5, (2[22m]/[30m]), assuming a center frequency of 50 Hz.

Directional arrays, frequency windows, and bias level controls allow recorder gains to be adjusted in such a fashion that the printed record is most pleasing to the eye, and, perhaps, a bit easier to interpret. But in actual practice, the lineup of events and reflector quality, those factors which enhance visual correlation, are the only signal/noise improvement factors that are really significant. If the noise contaminant comes from directly beneath the hydrophone array (multiples, diffractions, etc.), then the experience and intuition of the analyst becomes the final available filter.

V. GEOMETRICAL AND ENVIRONMENTAL INFLUENCES ON RECORD INTERPRETATION

The continuous seismic reflection profiler is a powerful tool for unraveling details of geologic structures and the distribution of probable rock types beneath the ocean floor. However, the system does not provide unique solutions to these complex interrelationships because the nature of the equipment and the complexity of sound waves transmitted over long distance through a varying medium do not allow simplifying assumptions. Therefore, the intent of this section is to point out some of the spurious events that appear on the record, interspersed with true reflections, and which must be accounted for before the full usefulness of this instrument can be realized. For a fully unique solution to geologic complexities, other types of data, such as drillhole samples and magnetic and gravimetic field intensities, must be considered.

A. RAY PATHS

Energy can follow at least six different ray paths between the source and receiver (Figure 6). All of these paths carry information that contributes to the interpretation of seismic profiles. The direct ray's slant range can be determined if the depths of, and horizontal distance between, the source and the receiver are known. By the geometric relationship $[(\text{source depth} - \text{receiver depth})^2 + (\text{distance})^2)]^{1/2}$, the slant range can be calculated. This value, when divided by an average surface water velocity, should be very close to the measured travel time, verify the source and receiver geometry, and identify a first event on the record. The path length of the surface-reflected ray may also be calculated; however, in deep water and with the relatively slow recording speeds used in single-channel recordings, this step is seldom necessary or easily accomplished.

Expected arrival times of the four bottom-reflected rays can be calculated from source and receiver depths, the water depth, and the assumption of near-normal incidence for the reflected rays. The first arrival should occur at a time determined by $([(Z-S) + (Z-R)]C)$, where (S) and (R) are source and receiver depths, respectively; (Z) is the water depth, and (C) is the average sound velocity in water. The second and third arrivals will occur at $[(2Z + S-R) \times (C)]$ and $[(2Z - S+R) \times (C)]$, respectively. These last two reflections will return simultaneously if the source and the receiver are the same depth (Figure 6). If these depths are adjusted to about one-fourth wavelengths of the center frequency, destructive interference would greatly diminish the intensity of the recorded signal, thus making the record easier to interpret. The fourth arrival occurs at $([(Z+S) + (Z+R)] \times [C])$. This return forms the end of a particular reflection sequence, which, dependent on the geometry, consists of three to four echo sequences.

In addition to the four bottom-reflected ray paths, most marine seismic sources generate one or more bubble pulses of varying intensity that contribute another group of ray paths similar to those shown in Figure 6. Filtering, which helps to isolate frequencies of maximum value, adds several harmonic oscillations to the wave train. Finally, the source energy is usually of such intensity that two or more source-bottom-surface round trips are possible. Thus, the problem in analyzing sub-bottom profiler records is essentially that of identifying the first of these many reflected arrivals from each sub-bottom reflecting horizons, and discarding the remainder.

B. IDENTIFICATION OF REFLECTED SIGNALS

As the source (air gun or sparker) discharges, an initial shock wave is generated. This shock wave, or pulse, has a rise time of only a few microseconds. Since it represents zero time for all practical purposes, this is the pulse whose progress is monitored to determine structure beneath the ocean floor. The various acoustic events following the initial pulse are identified in Figure 7.

Figure 7 is an example of a one-second sweep rate air gun record in which the arrival times of the various signals are noted. The 57-msec time delay represents the time between initiation of the sweep and arrival

of the signal at the hydrophone if the time interval between the beginning of the sweep and the discharge of the gun is neglected. Using a surface water velocity of 1.48 m/msec (estimated from Handbook of Oceanographic Tables, Naval Oceanographic Office, SP-68, 1966), the distance from source to receiver is 82m. This is a reasonable value because full deployment of the hydrophone array was not practical in this particular installation.

The surface-reflected pulse (Figure 6) normally follows the initial pulse with a time delay indicative of the total depth of the source and the receiver. In Figure 7, the 65-msec event suggests a receiver depth of about 9m and a source depth of about 1.5m, both of which are reasonable values for this installation. However, the fact that the 65-msec pulse and its bottom reflection both follow the initial pulse and its bottom reflection with no change in time delay, implies a greater degree of regularity than is likely for towed source and receiver. The increases in amplitude of the bottom-reflected counterparts of the 57- and 65-msec events indicate that the initial events were not in the plane of maximum sensitivity of the hydrophone array, while both reflected events were more nearly so. Most likely, the 65-msec event is an artifact of the outgoing pulse, and the slight variations in amplitude along the horizontal axis are due to the addition of a surface-reflected component.

Again, in Figure 7, the 77-msec event followed 12 msec later by another signal could possibly be caused by the initial pulse bouncing off the ship's hull and then off the water surface. This would mean that the gun was towed about 15m astern, and the total hydrophone distance was 99m. These are considered reasonable values for the particular installation used for this record.

The next three events (105, 139, and 167 msec, Figure 7) could be any number of things, such as surface duct multiples, reverberation from sound hitting the ship's hull, filter ringing, or bubble pulses. Reflections from the ship's hull appear on the record as low energy waves ahead of the bubble pulse, and frequently have a resonant character because the hull tends to reverberate. In addition, other repetitive noises aboard ship, such as paint chipping, heavy machinery, or radio transmission (Figure 5), can be received and recorded as interference, particularly if shipboard wiring is poorly grounded.

C. BUBBLE PULSES

Hydraulic afterflow, the temporary storage of kinetic energy not immediately radiated, is inherent in underwater explosions (Kramer et al., 1969). This afterflow is manifest as a series of oscillating bubbles. The size, the period of oscillation, and the identity and control of such bubbles are significant in the interpretation of marine seismic records. In general terms, the air from an air gun or the vapor generated by a sparker expand much more rapidly than they rise through the water column. This factor, coupled with the momentum imparted by the explosion, causes the pressure within the expanding gas bubble to become less than ambient pressure, much in the fashion of a ball containing three orthogonal springs which, from the compressed positions, are stretched past their equilibrium positions. At some diminished pressure, the process reverses and the bubble begins to collapse under the influence of the excess ambient pressure, and the reverse momentum generated by the implosion of the bubble analogous to the contraction of the orthogonal springs. The inward rush of water and the concurrent decrease in bubble size continues until the pressure inside the now-compacted air bubble is greater than the ambient pressure. Also, the ambient pressure is decreasing continually because the bubble is steadily rising through the water column. At this point, because of the elasticity of the compressed air within the bubble, the process reverses and a second expansion begins. These alternating expansions and contractions are called bubble pulse oscillations.

Bubble pulses generate compressional waves within seismic frequencies, and continue to do so until the energy is diminished below the threshold of the receiving equipment or the bubble reaches the surface. In the case of a sparker source, only one bubble oscillation is recorded, because steam is formed by the discharge and degenerates to water on the compression cycle (Figure 2).

The air gun wave train in Figure 3 shows three bubble oscillations from a depth of 4.6m. Not only does the energy diminish rapidly with each bubble oscillation, but the period becomes smaller. Energy is lost by turbulent waterflow and other related effects which tend to decrease bubble size. In addition, smaller bubbles rise faster because they must move less water, and thus oscillate fewer times (Kramer et al., 1969).

Factors involved in determining bubble pulse periods are charge size and depth of explosion. These parameters are related by the empirical formula $T = [0.000209(KQ)^{1/3}][(d + 33)^{-5/6}]$, where (T) is bubble pulse period in seconds, and (d + 33) is a depth factor in which (d) is the source depth in feet and (33) is the atmospheric pressure correction factor. (K) is a constant equal to 1×10^{10} and 1.36×10^{7}, when (Q), the potential energy of the gas bubble at maximum radius, is expressed in kilojoules (sparker), and foot-pounds (air gun), respectively (Kramer et al., 1969). Based on their data, a (Q) value of 40×10^{3} foot-pounds was approximated for the 10-in^3

air gun used for the record in Figure 7. A decrease in air gun operating pressure decreases the bubble pulse period.

The 139-msec event in Figure 7 is undoubtedly the bubble pulse. If the source is a 10-in^3 air gun pressurized to approximately 800 psi and towed at 1.5m depth, then the bubble pulse period would be about 82 msec, and its arrival time at the hydrophone array would be 57 msec + 82 msec = 139 msec. The width of the return at 139 msec would probably obscure the surface reflection of the bubble pulse even if the bubble did not vent to the surface on the first oscillation as is probable with only a 1.5m source depth. A high-speed recording oscillograph is usually required to resolve the surface reflection of a bubble pulse (Figures 2 and 3).

D. MULTIPLES

One of the consistently difficult problems in interpretation of single-channel seismic profiles is the identification and elimination of multiple path arrivals. The bottom-surface-bottom multiple is usually relatively simple to identify. For example, the bottom return (area on left side of Figure 7 arrives at 266 msec, and the first bottom multiple is very likely the strong echo at 514 msec. The 18-msec difference between the times required for two surface-to-bottom round trips is undoubtedly due to shortening of the multiple's vertical path length relative to the primary's vertical path length, because of the more nearly vertical angle of incidence of the multiple reflected signal. Other factors that confirm the 514-msec event as the true bottom-reflected multiple are the characteristic repetition of shapes and the doubling of apparent dips (Figure 7).

Intrabed, or "peg-leg", multiples are more difficult to identify than bottom-surface-bottom multiples. A simple rule of thumb in visual identification of an internal multiple is to look for changes in position of a reflector with respect to the position of its suspected multiple. The suspected multiple should be parallel to the primary reflector but displaced in time. This rule of thumb should be used judiciously, because velocity variations between layers can cause apparent displacements (Figure 8).

Although deep scattering layers and water inhomogeneities may produce multiples at frequencies commonly used for depth soundings, the interference of these factors is unusual at seismic frequencies. Nevertheless, strange events may be recorded for which no source is readily apparent (Figure 9). The multiple event in Figure 9 is possibly some malfunction of the equipment, some unrecorded peculiarity in the geometry of the installation, or even a flaw in the recording paper. Its effect on the record is obvious.

Qualitative visual analysis is usually limited to the interval between the first bottom echo and the first bottom multiple. Digital data processing techniques are required for complete multiple suppression.

E. VELOCITY EFFECTS

Compressional wave velocities in oceanic sedimentary and volcanic rocks vary both in horizontal and vertical directions. These velocity variations may cause some inconsistencies in record interpretation unless an allowance is made for their effects.

Low-velocity layers within the stratigraphic column have long plagued terrestrial seismologists (Thompson, 1963). Figure 8 shows schematically the effect of thickening and thinning of low-velocity layers on the reflected record section. This figure illustrates that apparent thinning can be produced by increasing either thickness or velocity above a given horizon. For example, the apparent dip of reflectors underlying the head of Oceanographer Canyon (Figure 7) is undoubtedly exaggerated by the increasing depth of water — a thickening low-velocity layer in this case — over the canyon axis.

Similarly, reflectors along the edge of a declivity, such as a canyon wall or slope break, will appear to downbend prior to outcropping when, in reality, these reflectors may outcrop horizontally. The reason is the same; as the bottom slopes downward, the thickness of the slower water path increases while the faster sediment path remains the same. The result will be longer arrival times and an apparent downbending of the reflectors. To determine if velocity variations might be real cause for these effects, the reflections must be corrected for interval velocities and replotted to true scale (i.e., without vertical exaggeration).

Vertical velocity variations can have a profound effect on the apparent shapes of erosional channels and true synclines when these features are displayed on a seismic time section. For example, the apparent syncline at Point A in Figure 10 is very likely to be a true structural feature. Close examination of the reflectors beneath arrow (A) shows that dips become steeper with increasing depth, undoubtedly because the velocity increases with increasing depth, thus displacing successively deeper reflectors progressively upward on a time section. On the other hand, at point B in Figure 10, an apparent syncline lies directly beneath an erosional channel. Accepting the validity of the coincidence of a syncline beneath an erosional channel does not explain the

broadening of the feature with depth. The broadening of the apparent syncline with depth is due to the downward displacement in time of reflectors in response to the increased thickness of the low velocity water layer in the channel, thus resulting in a structure which is the artifact of a velocity anomaly (Tucker and Yorston, 1973).

Velocity variations may cause apparent thinning or apparent dip between reflecting horizons, faults that appear as folds, or horizontal reflectors that appear as gravity slides on the recorded time sections. Tucker and Yorston (1973) maintain that the vagaries of geology are such that any coincidence of surface, near-surface, and subsurface reflectors is sufficient to suspect velocity inconsistencies.

F. DIFFRACTION EFFECTS

A diffraction is the echo pattern produced by energy scattered from a sharp peak, edge, or similar irregularity. Diffractions (side echoes) can cause small, sharp, erosional valleys and synclines to appear to be underlain by anticlines (Figure 11). A diffraction and an anticline can be distinguished because a diffraction is hyperbolic in that its maximum curvature is at the highest point and flattens out uniformly with depth. This situation exists because the point of origin of the diffraction does not move as the observation point is moved along the surface, whereas the apparent reflecting point moves in response to changes in receiver position. The limbs of a true anticline will appear to become less steep with depth because of the normal increase in velocity with depth (Tucker and Yorston, 1973). To detect these differences, the depth section should be replotted without vertical exaggeration because vertical velocity increases cause apparent decreases in vertical exaggeration.

Diffracted water wave arrivals may cause structures that appear as diapirs on the record (Ball, 1969). Diffracted water wave signals are common and may be of sufficient amplitude to obscure the configuration of reflectors beneath the apparent diapir if the reflector is restricted in area. To determine if a diapir is real or is a restricted area reflector, square the shallowest water depth over the crest of the suspected diapir, and add this quantity to the square of the horizontal distance from the crest to the ship's position. If this sum approximately equals the squares of the water depth directly beneath the ship at the horizontal distance used, then the feature is very likely an artifact of diffracted water wave arrivals (Ball, 1969) (Figure 12).

In the case of a true intrusive or diapir, the actual width of the structure will be obscured by diffractions and weak reflections that occur within the length of the hydrophone array. Normally, lack of alignment of reflectors appearing within the length of the hydrophone array should present no problem except in very shallow water. For example, in 1-km water depth, the difference in arrival times between a sound wave at the first hydrophone in a 22m-long hydrophone array towed 183m behind the ship, and the last hydrophone in that array, is 0.7 msec (assuming straight line propagation and 1.5 km/sec velocity). On a record in which one second of the vertical scale equals 119mm, this time difference equates to 0.08mm of record length. In deeper water, the time differences would be less.

The edge of the intrusive is always somewhere inside the apparent limits of the structure. This situation is particularly obvious in cases where basement relief apparently preceded the sediment cover. Then the horizontally layered sediments will appear to have penetrated the sides of the basement high, when, in reality, side echoes from the basement high are simply arriving ahead of the true sea floor reflections (Figure 13). Krause (1962) developed equations for determining horizontal displacement of a diffracted arrival if the apparent slope of the feature producing the diffractions and the depth of the flat sea floor are known. Near point A in Figure 13, the highest part of the flat sea floor is approximately 4780m below sea level, and the apparent slope of the lower part of the intrusive is 15.5°. Using these parameters in the equation $\overline{IJ} \simeq Z_3 X \tan \theta$, for dips of less than 30°, the horizontal displacement of the side of the intrusive is approximately 660m (4780 X tan 15.5/2), where $\overline{IJ}$ is horizontal displacement, Z_3 is the depth of deeper flat bottom, and tan θ is the apparent dip (Krause, 1969, Eq. 37A). With a ship's speed of 18 km/hr, diffractions from the intrusive begin arriving ahead of the true sea floor reflection about 2 minutes before the actual contact between the sea floor and the intrusive is reached. For slopes greater than 30°, it is necessary to convert apparent slopes to true slopes as illustrated in the section on dip calculations (p. 15).

Because the insonified area of the bottom and sub-bottom is rather large, signals reflected from surfaces outside the plane of the profile will appear on the profile at apparent depths much greater than their true depths. In addition, reflections from dipping beds are shown as if their arrival paths were vertical rather than perpendicular to the reflector. The result is that the actual locations of dipping reflectors are updip, and shallower than they appear to be from the seismic profile (Ball, 1969). The best way to evaluate these phenomena is to run closely spaced lines with frequent cross-checks.

G. AMPLITUDE EFFECTS

The 23-dB dynamic range claimed for the recording papers used with facsimile recorders effectively adds a z-component to standard X/Y coordinate recorders. The intensity of the z-component is a qualitative measure of the amplitude signals arriving at the hydrophone array. The displayed amplitudes represent reflecting horizons which, in turn, are approximately equal to lithologic interfaces, and therefore are subject to lateral variations in both form and composition. Thus, even relative amplitude variations are capable of revealing a great deal of additional geological information if amplitude anomalies due to the instruments used and those due to operational geometry can be separated from the total returning energy.

Relative amplitudes may vary in response to source strength and directivity or to receiver coupling and directivity. The signal emitted by the source is capable of shot-to-shot variation. In the case of a sparker, bits of electrodes are spalled with each shot; electrode deterioration can become noticeable after an extended period of operation. The result is a gradual decrease in output energy which appears on the recorder as a gradually decreasing signal. To ameliorate electrode deterioration, the polarity of the electrodes must be changed. Before further evaluation of a relative amplitude change on a sparker record, the operational log should be examined to determine elapsed time since the most recent polarity check.

Similarly, source and receiver depth changes may reinforce or diminish reflected energy by increasing the bubble pulse period and constructively or destructively reinforcing reflected signals.

According to Schoenberger and Levin (1974a), when a seismic wave passes through a cyclic section of sediments, the initial pulse is broadened by the generation of a set of intrabed multiples. The lower order multiples have the same phase as the initial pulse and tend to add energies at the lower frequencies. In addition, as the beds become thinner, the amplitude of the reflection will decrease because amplitude is proportional to thickness, but inversely proportional to wavelength (Widness, 1973). Owing to the vertical geometry of the reflectors, some echo sequences may appear on the record with amplitudes that are not related to the physical properties of the sediments in the section.

In addition to frictional absorption, the interfering multiples, and other physical peculiarities, the inherent low passband nature of the earth leads to diminution of reflected energy. The proportion of low-frequency energy in the reflected passband increases as reflector depth increases, because the earth selectively attenuates the higher frequencies, thus reducing the overall signal level. After all identifiable sources of amplitude variations related to operational procedures and signal peculiarities have been resolved, those anomalies remaining are very likely to have some measure of geologic significance.

Acoustic energy may converge when reflected from a concave surface or diverge when reflected from a convex surface, thus producing high- and low-amplitude reflection sequences, respectively (Figure 13). Convergence and divergence are qualitative measures of sub-bottom roughness because signal scattering occurs when sharp local relief (roughness) is greater than the wavelength of the signal divided by eight times the cosine of the angle of incidence (Leong et al., 1971). Although all surfaces are acoustically smooth at normal incidence (cosine of the angle of incidence becomes 0), all seismic energy may not reach the reflecting surfaces at normal incidence, resulting in variable intensity echoes because of variations in scattering (Figure 13).

Scattering, lateral variations in reflector lithology, cementations, and diffracted water wave arrivals from faults and point reflectors may all appear on records as variations in relative amplitude which may assume a variety of geometric shapes. For example, pagoda structures noted in the eastern Atlantic (Emery, 1973) and in other areas may be due to these factors, because 3.5 kHz sound waves may be scattered or coalesced by roughness features of less than 2m relief (Leong et al., 1971).

Structural or facies relationships may be better understood by the consideration of qualitative amplitude data (Lamer et al., 1973). For example, strong reflections from the evaporitic sequence overlaying a salt dome may help distinguish it from a shale dome or a depositional anticline. Marker horizons may be traced and correlated over widely separated areas on the basis of a characteristic reflected signal, one component of which is relative amplitude. Horizon A, a widespread sequence of closely spaced chert beds in the North Atlantic, is a well-known example of this phenomenon.

At a reflecting boundary, the Rayleigh reflection coefficient, a quantitative measure of amplitudes, is the ratio of the acoustic pressures of the incident and reflected waves. At normal incidence, the reflection coefficient (R) is determined from the expression

$$\frac{\rho_2 V_2 - \rho_1 V_1}{\rho_2 V_2 + \rho_1 V_1}$$

in which ρ_1, ρ_2 and V_1, V_2 are the densities and velocities in the upper and lower layers, respectively.

Hamilton (1970) calculated reflection coefficients for a variety of bottom sediment types in three geological environments and derived values between 0.4098 for a coarse-grained continental shelf sand, and 0.0941 for an abyssal plain clay. Reflection coefficients are linearly related to porosity by the equation $R=0.6468-0.6456(n)$, in which (R) is the reflection coefficient and (n) is porosity (Fass, 1969). Extremely high reflection coefficients for unconsolidated sands have been related to occurrences of natural gas; the reflection coefficient is a measure of fluid saturation because porosity and saturation are inversely proportional to velocity, but directly proportional to density. The sea floor is normally a good reflector because the large increase in densities more than offsets the small velocity variations across the water/sediment interface. Reflection coefficients decrease with depth because the magnitudes of layer-to-layer density/velocity variations decrease with increasing depth. Reflection coefficients can be estimated qualitatively from normal incidence seismic records when the first layer ($\rho_1 V_1$) is of low velocity and low attenuation because the reflection coefficient is frequency independent and is determined by the ratio between direct and reflected peak amplitudes (Hastrup, 1970).

H. DIP CALCULATIONS

In areas of constant slope, the recorded dip of bottom and sub-bottom reflectors is less than the true dip of these reflectors (Krause, 1962). However, the tangent of apparent dip is approximately equal to the sine of true dip up to about 15° when the ship's track is parallel to the direction of true dip. Most oceanic structures have dips less than 15°.

When the relationship is between ship's track and true dip is unknown, and the apparent dip is greater than 15°, then it is necessary to correct for both ship's heading and apparent dips. The best approach for determining these factors is to calculate apparent dips and track heading at points where record sections intersect, and from these data, calculate true dip in the manner described by Brooks (1970).

Data available at the point of intersection of two tracks are apparent dip and ship's heading for each record. From the geometric relationship, the tangent of the apparent dip is equal to the tangent of the true dip times the cosine of the difference between ship's heading and true dip direction ($\tan \S' = \tan \S \cos \beta'$ in Brooks' terminology). Of these parameters, only the tangents of apparent dip can be determined from the record, so it is necessary to define two other parameters.

One of these, (δ), is the ratio of the tangents of the apparent dip angles from each profile ($\delta = \tan\S'/\tan\S''$); and the other ($\eta$), is the cosine of the angle separating the two headings or ($\eta = \cos(\beta' + \beta'')$) (Brooks, 1970). With these values, it is possible to calculate $\cos\beta'$ and $\cos\beta''$, wich are the variations of each track from true dip direction, and then substitute these values into the true/apparent dip relationship. These values are calculated from

$$\text{Cos}\ \beta' = S[(1-\eta)/(1-2\eta\delta + \delta^2)]^{1/2}$$

$$\text{Cos}\ \beta'' = [1-\eta^2/(1-2\eta\delta + \delta^2)]^{1/2}$$

which are Brooks' equations 7 and 8, respectively.

For a numerical example, assume that the apparent dip measured on a track bearing 345°T is 24° at the point of intersection, with a track bearing of 015°T, and having an apparent dip of 18°. The first step is to calculate δ from $\tan\S'/\tan\S''$ (.4452/.3249 = 1.3703), and then η, which is $\cos(360-345) + (15-0) = \cos 30°$. Using these values to find $\cos\beta'$ (Brooks Eq. 7) and $\cos\beta''$ (Brooks Eq. 8) yields 0.70631 and 0.49564, respectively. Finally, substituting in $\tan\S = \tan\S'/\cos\beta'$ (0.4452/0.70631 = 0.63032) gives the angle of true dip as 32.22°, and $\tan\S = \tan\S''/\cos\beta''$ (0.32492/0.49564 = 0.65555) gives the angle of true dip as 33.25°.

I. VERTICAL EXAGGERATION

Because the ordinate of the seismic strip chart recorder represents depth through the water column in seconds, and the abscissa represents distance over the ground in hours, some scale adjustment must be made. Vertical exaggeration, the ratio of horizontal scale to vertical scale, is one measure of this scale disparity.

Vertical exaggeration is calculated by referencing vertical and horizontal scales to unity. For example, in Figure 13, one hour of ship's travel time (horizontal scale) is equal to three cm of record length, or 16,470m ground distance. On the vertical scale, 0.5-second travel time is also equal to three cm record length, or 366m uncorrected depth. HS/VS is approximately equal to 45:1, which means that the vertical scale is expanded 45 times relative to the horizontal scale.

The effect of vertical exaggeration is to foreshorten distances and distort the width of features relative to their height, thus making gentle rises appear as precipitous slopes. Conversely, some degree of vertical exaggeration is necessary in order to recognize features that would likely be missed without some added emphasis. If true dips and surface gradients are to be determined, the effects of vertical exaggeration must be removed either by replotting the record at a 1:1 scale, or by dividing the tangent of the apparent slope by the vertical exaggeration to obtain the true tangent of the slope.

When correlating from one record to a record made on a different cruise, one must be aware of the effects of scale differences. This is primarily the reason for operating one recorder at a fixed sweep rate.

J. RESOLUTION

Resolution is the minimum time between reflectors that can be reliably measured from the record. Ultimately, a complex interrelationship between reflector spacing, filter bandwidth, signal/noise (S/N) ratio, velocity/depth profile, source characteristics, and recording speed determines the minimum reflector thickness that can be resolved. Some of these factors can be quantitatively evaluated. Others, such as the S/N ratio, are qualitative and must depend on the experience and intuition of the analyst for meaningful evaluation.

According to Ricker (1953), the individual wave components of a seismic wave train are resolvable only when similar phases are separated in time by an amount greater than 0.428 of the time period of the wave. Based on this observation, the minimum resolvable reflector thickness is $h = (0.428V/2f)$, where (V) is sound velocity in the sediments and (f) is the dominant frequency. For the case in which the sound speed is 1.5 km/sec and the center frequency is 50 Hz, the minimum resolvable layer thickness would be 6.42m.

However, on a 4-sec sweep speed seismic record, one second of one-way travel time is represented by 119.06mm of record width. At that scale, 6.42m is represented by approximately 1.01mm. Under the most favorable S/N conditions, approximately 7m would be the minimum resolution if the outgoing signal were a single pulse.

The reflection group indicative of a single interface is made up of at least four separate events exclusive of the bubble pulse and its associated surface reflections (Figure 6). If an average sparker bubble pulse time period of 0.025 sec is assumed, then the onset of the bubble pulse event will occur at 2.98mm (0.025 sec × 119.05), after the beginning of the initial pulse. In addition, if the bubble pulse has all the ray paths shown in Figure 6, then an additional 0.008 sec (Figure 2) will elapse before the beginning of the last part of the signal. This time delay is equivalent to a record length of about 1mm. Thus, the total distance across the record corresponding to the initial wave train is approximately 4mm, which equates to about 0.017 sec one-way travel time (4/119.06/2), or approximately 25m at an assumed sound speed of 1.5 km/sec.

Frequently, the bottom return will be considerably wider than 4mm without being degraded by adverse S/N ratio. In this case, it is safe to infer that layering exists in the upper 25m, but it is often not possible to determine how many layers are present or how much they are separated.

The velocity/depth relationship is capable of affecting both the amplitude of the recorded signal and the reflector separation that can be resolved. For example, under the influence of a positive density/velocity product (ρc) gradient, reflectors separated about ¼ λ (wavelength) (about 7½ m for 50 Hz at 1.5 km/sec) will add constructively to produce a return of higher amplitude than either of the component echoes. However, for a negative ρc product gradient (Figure 14), reflectors separated about ¼ λ will add destructively and the total amplitude will be reduced.

These amplitude variations occur because a reflection that returns from a boundary characterized by an increase in ρc product will have the same phase as the initial signal striking the boundary. Conversely, when the structure of the ρc product is such that the overlying layer has a higher ρc product than the underlying (Figure 14), then the seismic waves reflected from either surface of the layer will have different phases. These reflections sum differently from reflections with similar phases. For normal incidence waves, the phase shift will be 180° when the transmitting medium is high density/high velocity (water), and the medium across the reflecting interface is low density/low velocity (air).

Widness (1973) has noted that a reflector ⅛ λ (¼ λ separation) thick is capable of returning constructively interfering echoes from both its top and bottom surfaces if the velocity gradient is negative (Figure 14). The ⅛ λ is defined as the minimum thickness capable of supporting signal coherence at seismic frequencies. However, for 50-Hz reflections, ⅛ λ is about 3.25m, and the time difference between top and bottom reflections would be 0.004 sec [(2) × (3.25m/1.5km/sec)]. This time difference equates to 0.5mm, and is not reliably

resolvable from the record. As noted previously, about 25m of sub-bottom reflection time (4mm on the record) is required to encompass an entire wave train. If a single cycle of the predominant frequency (50 Hz) is 30m long, it is unlikely that a portion of a single cycle will ever be recorded, or that constructive or destructive wave interference will be a recording problem.

VI. GEOLOGIC INTERPRETATION OF SEISMIC RECORDS

Sub-bottom layers reflect sound waves in a manner which depends on the wavelength of the sound and on the physical and chemical characteristics and configuration of these boundaries. In this context, reflections occur at sharp boundaries representing facies changes or lithification changes, or at chemical or physical phase transition boundaries. Thus, the purpose of this section is to establish criteria by which these boundaries may be qualitatively differentiated on records which represent only the apparent traveltime of sound between reflecting horizons. Attenuation is the measure of energy lost when a seismic wave travels through various media. These energy losses are due to absorption by the material, scattering by the shape of the insonified surface, reflections and refractions at the boundary, and spherical spreading of the compressional wave. Because attenuation is a function of frequency (Hamilton, 1970), wavelength of energy penetrating the bottom is continually increasing downward. This situation produces two related effects: (1) the thickness of an interface required for producing a reflection will increase, and (2) the scale of relief necessary to scatter signals must also increase. As a result, the terms "acoustically rough" and "acoustically smooth" are very qualitative. In other words, a buried transparent layer may be quite different geologically from a transparent layer at the surface.

Despite these restrictions, many acoustic properties are related to changes in geologic regime. For example, Figure 15 shows reflections related to vertical bedding change, angular unconformity, disconformity, structural deformation, crossbedding, onlap, erosion, and slumping. The descriptions that follow reflect the geologic history of the Canary Basin and may not be applicable in other areas; nevertheless, a classification should be established as a first step in geologic interpretation.

A. UPPER ACOUSTICALLY TRANSPARENT ZONE

West of about 27°W in the Canary Basin, the upper sediment interval is acoustically transparent to frequencies of 20 to 125 Hz. This zone is without internal reflectors, remarkably conformable to sea floor topography, ranges up to about 0.25-sec, two-way travel time in thickness, and decreases to an unresolvable thickness on the lower edge of the continental rise, (point A, Figure 16).

On the seismic profiler record, the transparent layer appears completely devoid of structures. However, at high frequency (3.5 kHz) and greater vertical exaggeration ($\simeq$ 20:1), the surface appears to be displaced downslope by creep or other type of mass movement (Figure 17).

Well logs from Joides drill site 137 describe the upper 58m of sediment as a nonfossiliferous brown clay consisting of terrigeneous minerals, mainly quartz (Hayes, Pimm et al., 1972). These sediments have undoubtedly accumulated particle by particle, by settling through the water column, and suggest long-term tectonic and oceanographic stability because some deep topography has been completely damped at the surface. In some fashion, the distribution of these sediments is related to topography because the transition from some transparent to stratified areas appears relatively abrupt.

B. STRATIFIED ZONE

Upslope on the African Continental Rise to the east of about 27°W and in locally isolated basins atop the transparent layer, bottom sediments consist of a series of closely spaced reflectors (point B, Figure 16). Close spacing of these reflectors produces an almost opaque appearance on the record. This zone has a maximum thickness in excess of 1.0 sec (two-way travel time) upslope, but decreases downslope to 0.1 sec or less. In many cases, these reflectors appear to conform to underlying structures; in other cases, they appear to be confined to structural lows (Figure 16). At Joides drill site 138 (Hayes, Pimm et al., 1972), the upper sediments are described as a 150m section of green and brown silty and sandy clays interspersed with grayish-green sand layers. The sand is fine-grained, well-sorted, and apparently terrigeneous or locally volcanogenic. Locally, this material may be turbidites because of the well-developed stratification and the contemporaneity with the transparent zone, but it is also very likely that a great deal of this material was transported by saltation, sheet flow, slumping, and reworking by bottom currents.

C. LOWER ACOUSTICALLY TRANSPARENT ZONE

Throughout the Canary Basin, the layered zone is underlain by another acoustically transparent zone.

Its thickness can be greater than 1.0 sec over particularly deep portions of the underlying topography. In a few locations, the layered zone rests directly on the underlying topography, and the lower transparent zone has been eroded or not deposited.

The lower transparent zone is present at Joides drill sites 137 and 138 (Hayes, Pimm et al., 1972). The lowermost sediments are described as silt-free, nannomarl and chalk ooze, and thin foriminiferal sand layers (site 137), and dolomitic lutites, reddish-brown semiconsolidated clays, and massive mudstones (site 138), but without quartz. The layering is quite likely too thin to be resolved by sound of wavelength that penetrates to these depths.

D. DEEPEST OBSERVABLE REFLECTOR

Except on the continental rise, seismic penetration was always ended by a series of high amplitude echoes which are loosely labeled "basement" by most observers. However, detailed examination shows two distinct types of reflections that undoubtedly indicate two types of basement.

One type of basement is characterized by a relatively smooth upper surface and the faint suggestion of layering (point D, Figure 13). At Joides site 138 (Hayes, Pimm et al., 1972), a coarse-grained, intergranular, alkalic basalt was identified as basement and interpreted as an intrusive sill. This leads to speculation that a good portion of the smooth basement is actually an intrusive or a series of low-viscosity flows that incorporated existing sediments. Figure 18 supports this latter conclusion, because it is one of the few sections which shows well-defined "basement" reflectors beneath an acoustically rough "basement" surface. It is concluded that smooth "basement" is likely to be basaltic flows or indurated sediment.

The second type of basement is characterized by high-amplitude, reverbatory reflections indicative of a rough surface with rugged relief (point D, Figure 16). In many cases, overlying sediments are conformable to this surface, while in other instances, relief is muted by the overlying beds. Relief may range between 0.1 sec and several seconds. Where high-amplitude, reverbatory "basement" has been dredged or drilled, it is usually some type of basic or ultrabasic igneous rock, and where it is present, no deeper reflectors are observed. Where neither of these types of reflectors are present, depth to basement should not be recorded.

E. SEDIMENT PATTERNS AND GEOLOGIC MODELS

The vertical and horizontal patterns of distribution of reflector types contribute to development of models indicative of structural and sedimentary history. For example, closely spaced stratification may be interpreted as turbidites unless they occur on a relatively steep slope or undulate over basement topography that has not been subjected to secondary deformation. In this case, the closely spaced acoustic stratification may be caused by changes in lithification, sedimentation rates, or grain sizes with depth.

Depressions ringing basement highs may be indicative of bottom current accelerations around obstructions or of isostatic depressions of the crust. Comparison of the thickness of the pelagic sediment cap overlying the basement high with the thickness of pelagic sediment away from the high may permit an estimate of the time period that the current has been active, if a sedimentation rate can be approximated. However, if the basement peak crests are completely bare of pelagic sediments, then either a strong bottom current is operative or the peak is a relatively recent tectonic feature. If the basement peak is suspected to be a recent feature, then examination of sediment-rock contacts should show that either the beds appear to overlap the sides of the feature (Figure 13), implying that the peak existed first, or that the track is not directly over the crest. On the other hand, if the beds close in to the basement peak are disturbed, thin individually, or appear to blend into the flanks of the peak, then the peak may be an intrusive, and is very likely younger than the sediments.

If the surface level of sediments on opposite sides of a basement feature are different, then the possibility exists that the feature is elongated and acted as a sediment dam. Alternatively, the levels may have been offset by faulting and volcanic intrusions (Figure 16). If this latter situation is suspected, then look for thinning of individual reflectors or other evidence of offsets in the stratigraphy. If sediment damming is the chief suspect, then sediment types should be different on opposite sides of the feature, i.e., acoustically transparent sediments should be thicker below the dam. Many of these distinctions are subtle and require a great deal of care to discern, nevertheless, seismic profiles are the best way to determine existing stratigraphic and structural relationships in two dimensions.

VII. VELOCITY GRADIENTS AND DEPTH CORRECTIONS

If a geological model of the ocean floor is based solely on normal incidence seismic reflection records, it must be considered semi-quantitative, and, thus, speculative, because of the lack of velocity, density, or other

mass physical property data for the sediments. To convert raw reflection data (time sections) to geophysical cross-sections representative of true depths to reflecting horizons, corrections must be made for the variations of velocity with increasing time within the sedimentary section. Once the velocity model is established, additional meaningful inferences about the physical properties of the sediments may be made.

Velocity gradients are the rates of change of compressional wave velocities with increasing depths. Gradients are usually expressed as an increase in velocity per linear increase in depth or sec $^{-1}$. In the upper levels of deep ocean marine sediments, these gradients are positive and usually lie between 0.5 and 2.0 sec $^{-1}$ (Houtz et al., 1968).

The purpose of this section is to show how data from other sources may be adapted for determining velocity structure. Joides drill site 138, located at 25°55.37'N, 25°33.79'W, will serve as an example for compilation of a bottom velocity model, because it contains all the necessary parameters to establish a velocity model and some independent measurements against which the model could be verified. LYNCH cruise LY-33A made two crossings of this drill site and detected four persistent reflectors at 0.070, 0.180, 0.250, and 0.460 seconds two-way travel time (Figure 19). If the seismic reflection record is interpreted with an assumed sound speed of 1462.8 msec (nominally 1/800 sec/fm assumed by most recorders), then the apparent depth of the reflectors below the ocean floor will be 1,462.8 × (travel time/2), which equals 51, 132, 183, and 336m, respectively. A check of the coring log for this site (Hayes, Pimm et al., 1972) revealed that a zone of silty clay and sand, identified as early Miocene, extended from 52 to 61m, that no stratigraphic horizons could be identified near 132m, that between 175 and 183m depth the rate of drilling decreased dramatically indicating a harder layer of clay, that an indurated mudstone with chert layers was encountered near 240m, and that basalt began at 435m below the water/sediment interface (Figure 19). Since the correspondence between apparent reflector depths and drilled depths is poor below 51m, the conclusion may be drawn that vertical velocity changes occur with increasing depth within the sediment column.

To establish sediment velocities that will permit apparent depths shown on the reflection record to be compared with drilled depths, interval velocities must be calculated by dividing drilled depth by the one-way travel time of the appropriate reflection. After calculating interval velocities along the drill hole, the following assumptions are made:

(1) The 0.070-sec reflector corresponds to the lithologic unit encountered at 52m, therefore, an interval velocity of 1.486 km/sec is appropriate (Figure 19).

(2) The reflector, at an apparent depth of 132m below the ocean floor, is an artifact of a gradual change in sediment physical properties or of inexact interval velocity; however, if the abrupt change in drilling rates at 156m represents an impedance mismatch of sufficient magnitude to produce a reflection, the calculation of an internal velocity between 52 and 156m or 1.891 km/sec is permitted.

(3) The indurated clay zone beginning at 175m may be related to the 0.180-sec reflector, although no reasonable interval velocity will account for the time differences between the 0.070, 0.180, and 0.250 reflections. A sonic velocity measurement for the interval between 183 and 190m made on board the GLOMAR CHALLENGER reports a velocity of 1.823 km/sec (Hayes, Pimm et al., 1972; table 4, p. 141). An instantaneous velocity calculated for this depth is 1.836 km/sec; the difference between these two values is less than 1%.

(4) The reflection arriving at 0.250 sec may be due to the same lithology that produces the drilling rate changes near 250m or the top of the indurated mudstone with chert layers found at a drilled depth of 255m. The interval velocity within this zone is 2.657 km/sec, which may be excessive.

(5) The basement reflection arrives at 0.460 sec, and is representative of the basalt encountered at 437m below the water/sediment interface. The interval velocity in the zone between the 0.180 and the 0.460 reflectors is 2.007 km/sec.

Given interval velocities and reflection times, the only other parameter required for completing the bottom velocity model is the initial velocity or velocity at the water/sediment interface. Although no velocity measurements were made by GLOMAR CHALLENGER at the water/sediment interfaces, Hamilton (1970) details a technique for very accurately relating initial sediment velocity (V_0) to the velocity of the bottom water if the sediment type can be inferred. According to Hamilton, the ratio of sound velocity in seawater to sound velocity in sediment can be considered a constant for a particular bottom sediment type, because the only changes in sound velocity in the bottom water and sediment pore water are due to temperature and pressure changes. Temperature and pressure effects on the mineral grains are inconsequential, thus, both water and sediment velocities can be corrected to in situ conditions and the ratio between these velocities will be constant. For example, a pelagic silty clay from an abyssal hills area has a water/sediment interface velocity ratio of 0.985, a clayey silt from an abyssal plain has a velocity ratio of 1.003, and a silty clay from a slope environment has a velocity ratio of 0.994 (Hamilton, 1970).

Joides drill site 138 is located near the foot of the African continental rise in an area where surficial sediments are described as green, silty clay with sand layers (Hayes, Pimm et al., 1972). The reflection profile across this site (Figure 19) shows a series of closely spaced reflectors which very likely approximate a silty clay continental slope environment. With this assumption and a bottom water velocity of 1515.8 msec at a depth of 5,288m (Naval Oceanographic Office, SP-68, 1966), the initial bottom velocity (V_0) at the water/sediment interface is 1.507 km/sec (1515.8 × 0.994).

To determine the velocity gradient (a) in the sedimentary section, the gradient equation developed by Houtz and Ewing (1963) is used. In this equation, $a = (\bar{V} - V_0)/\frac{1}{2}h$, the layer thickness (h) is divided in half because the instantaneous velocity ($\bar{V}$) is an average that is assumed to be representative of the midpoint of the layer.

Average gradient is the most practical parameter for correcting apparent depths to very nearly true depths. Thus, the average interval velocity for the entire section is 1.90 km/sec (437m[½(0.46 sec)]), and the average gradient is 1.799 sec^{-1} when V_0 is 1.507 km/sec.

To determine instantaneous velocity at any depth in the presence of a linear gradient, multiply gradient by depth and add to the initial velocity. For example, at a depth of 428m in Joides drill site 138, the calculated instantaneous velocity is 2.277 km/sec (V_0 = 1.507, h = 428m, a = 1.799 sec^{-1}). Between 425m and 431m, in drill site 138, three sonic velocity measurements in dolomite silts and carbonaveous muds averaged 2.369 km/sec (Hayes, Pimm et al., 1972; table 4, p. 141), or less than a 4% difference when compared with a value obtained by an average gradient method.

For correcting apparent reflector depths to more realistic depths, the linear gradient equation can be rewritten in the Houtz and Ewing (1963) format as $h = V_0(e^{at} - 1)/a$. With this equation, the depths to reflecting horizons as drill site 138 are 54, 147, 211, and 429m, respectively. Intervals at 147 and 211m were not cored, and the only indication of lithologic changes are slight changes in the drilling rate (Figure 19).

The calculated reflection depths permit two conclusions:

(1) Seismic reflections cannot always be correlated with lithologic horizons, and

(2) When an average linear gradient value is used to calculate depths, variations between true and calculated reflector depths will exist, especially as the sedimentary section becomes thicker. This latter situation occurs because gradients decrease with increasing depth in the sedimentary column. A more realistic travel time vs. velocity curve would show interval velocity decreasing downward as shown by Houtz et al. (1968).

As a rule-of-thumb, a linear gradient should be reasonably satisfactory to a one-way travel time depth of about 0.5 sec. Below that depth, a nonlinear gradient curve should be used if the considerable quantity of refraction data required for its construction is available; otherwise, the limitations of the results should be recognized.

VIII. DATA CONVERSION

Seismic reflection records, on which isopach and structural contour charts are based, are normally assembled from all available sources. As a result, these data are recorded at a variety of shot repetition rates, recorder speeds, ship's speeds, vertical exaggerations, and navigational accuracies. Prior to compilation, the analog records must be put into a digital format. One method of achieving this conversion is with an electromechanical digitizer, such as the Bendix 4-place X/Y digitizing table. However, this process introduces errors, the magnitude of which must be considered.

On the 10-second vertical scale record, the worst-cast — 10 seconds of two-way travel time — is represented by 3,818 digitizing table units along the record ordinate. This equates to approximately 0.955 table units per 1/4000-sec travel time, or one nominal fathom, the usual recorder scale. Consequently, one digitizing table ordinate unit is approximately 1.94m (1.047 fm). The record ordinates are always oriented to within ±2.5 table units. This means that elevation differences of 9.7m are distributed over the digitized width of the record, or that any single digitized value may have ±1m error because of record misalignment on the digitizing table. If the record length is 12h, thus representing 185 to 220 km, then the error introduced by acceptable alignment of the paper reduces to about 0.092 m/km of track.

Along the abscissa, 1 h of ship's travel time (150 lines per inch horizontal scale of the recorder) is equivalent to 483 digitizing table units. If a ship's speed of 16.7 km/h is assumed, then 30 table units represents 1 km. Abscissa orientation variances of ± 2.5 digitizing table units means that approximately 0.18 km will be distributed over the horizontal scale of the record section being digitized.

The other major source of digitizing error is identification of the onset of the reflection event. For the ocean floor event, several operator checks have shown a reading repeatability of ± 3 table units (5.82m). The onset of

basement and intermediate reflections are much more difficult to determine than the onset of the bottom event. As a result, the absolute depth to basement is estimated to contain as many as five digitizing table ordinate units of error. On a 10-sec vertical scale, 150 lines per inch of horizontal scale record (the maximum case), this equates to approximately 10m of vertical variation. Ultimately, it is the signal/noise quality of the record that controls the relative accuracy of the determination of reflection time; i.e., good records are easy to pick, poor records are difficult to pick.

After data points are scaled at unfixed, frequent intervals from the original record, they are averaged and compared at 3-min intervals. This means that data points are spaced at even time increments, but at variable distance increments. This procedure is unlikely to produce serious errors in the data because the difference between a maximum ship's speed of 18.50 km/hr and a minimum ship's speed of 12.95 km/hr is only 0.28 km. In fact, the averaging routine serves to smooth some of the vertical fluctuations or jitter introduced in the original data by the operator's placement of the cursor or the inconsistency of selecting the onset of deep reflections.

IX. SUMMARY

The question that remains after all the environmental, instrumental, and interpretational constraints have been considered is: Do the data present a unique and viable solution to a geologic problem? Although this question can never be precisely answered, the converse — what would be the effect of not considering these constraints? — can be approximated. For example, Figure 19 shows that a reflector could be mislocated by about 100m in 0.5 sec, two-way travel time, unless velocity data are used to correct to more appropriate depths. The effect of incorrect depths on sedimentation rate calculations or structural contours would be considerable. Similarly, failure to consider vertical velocity changes may also lead to interpretation of erosional features as synclines (Figure 10), or the derivation of unrealistic shapes for features beneath low-velocity layers (Figure 8).

An analysis which fails to account for diffraction effects could lead to imprecise location of the boundary between horizontal sediments and an emergent peak (Figure 13), the misinterpretation of side echoes as diapirs (Ball, 1969), or the conclusion that the sea floor is plunging beneath an oceanic trench. Even though reflector resolution of less than 7m is possible, the noise introduced by bubble pulse oscillations, secondary ray paths, and instrumental distortions reduces resolution to 25m or more. Other hazards to instantaneous correlations include variable vertical exaggerations, variations in amplitudes of reflected signals, and failure to reconcile differing reflection models wth different geologic regimes. Even though the drawbacks to collection and interpretation of reflection seismic data seem overwhelming, the seismic method remains the most rapid procedure for developing a reasonable and consistent quantitative geological model of the sea floor and its covering layers of sediments.

X. REFERENCES

1. Albers, Vernon M. (1965). Underwater Acoustics Handbook-II. University Park, PA, The Penn State Univ. Press., 290 p.

2. Allen, F.T. (1972). Some Characteristics of Marine Sparker Seismic Data. Geophysics, v. 37, p. 462-470.

3. Anderson, V.C. (1953). Wide Band Sound Scattering in the Deep Scattering Layers. Scripps Institution of Oceanography, San Diego, CA. SIO Ref. 53-36.

4. Ball, M.M. (1969). Discussion: Diapirs of Magdalena Delta. Am. Assoc. Pet. Geol. Bull., v. 53, p. 2195-2196.

5. Ballard, J. Alan and F.H. Sorensen (1968). Preglacial Structure of Georges Basin and Northeast Channel, Gulf of Maine. Am. Assoc. Pet. Geol. Bull., v. 52, p. 494-500.

6. Ballard, J. Alan and L. G. Hemler (1969). Structure of the Cape Verde Basin. Presented at 50th Annual Meeting of the Am. Geophys. Union, Washington, DC, Trans. Am. Geophys. U.

7. Bedenbender, J.W., R.C. Johnson, and E.B. Neitzel (1970). Electroacoustic Characteristics of Marine Seismic Streamers. Geophysics, v. 35, p. 1054-1072.

8. Brooks, M. (1970). Some Trigonometric Formulae for the Interpretation of Continuous Seismic Profiles. Int. Hydrog. Rev., v. 47, p. 65-72.

9. Brophy, J.J. (1966). Basic Electronics for Scientists. New York, McGraw-Hill, 471 p.

10. Emery, K.O. (1973). Review of the Results from the Eastern Atlantic Continental Margin Program of the International Decade of Ocean Exploration. Woods Hole Oceanographic Institution, Woods Hole, MA. WHOI Ref. 73-75, 21 p., unpub.

11. Evenden, B.S. and D.R. Stone (1971). Seismic Prospecting Instruments, Vol. II: Instrument Performance and Testing. Berlin, Gebrüderborn-Traeger, 195 p.

12. Ewing, J.I. and G.B. Tirey (1961). Seismic Profiler. J. Geophys. Res., v. 66, p. 2917-2927.

13. Fass, R.W. (1969). Analysis of the Relationship Between Acoustic Reflectivity and Sediment Porosity. Geophysics, v. 34, p. 546-553.

14. Giles, Ben F. (1968). Pneumatic Acoustic Energy Source. Geophys. Pros., v. 16, p. 21-53.

15. Hamilton, E.L. (1970). Reflection Coefficients and Bottom Losses at Normal Incidence Computed from Pacific Sediment Properties. Geophysics, v. 35, p. 995-1004.

16. Hastrup, O.F. (1970). Digital Analysis of Acoustic Reflectivity Tyrrhenian Abyssal Plain. J. Acoust. Soc. Am., v. 47, p. 181-190.

17. Hayes, D.E., A.C. Pimm et al. (1972). Initial Reports of the Deep Sea Drilling Project. Washington, DC, U.S. Government Printing Office, v. XIV, p. 135-156.

18. Horton, C.W., Sr. (1969). Signal Processing of Underwater Acoustic Waves. Washington, DC, U.S. Government Printing Office, 276 p.

19. Houtz, R.E., and J.I. Ewing (1963). Detailed Sedimentary Velocities from Seismic Refraction Profiles in the Western North Atlantic. J. Geophys. Res., v. 68, p. 5233-5258.

20. Houtz, R.E., John Ewing, and Xavier LePichon (1968). Velocity of Deep-Sea Sediments from Sonobuoy Data. J. Geophys. Res., v. 73, p. 2578-2596.

21. Junger, Arne (1964). Signal-to-Noise Ratio and Record Quality. Geophysics, v. 29, p. 992-995.

22. Knott, S.T. (1970). Operational Technique for Continuous Seismic Profiling and Related Studies. Woods Hole Oceanographic Institution, Woods Hole, MA. WHOI Ref. 70-43, 71 p., unpub.

23. Kramer, F.S., R.A. Peterson, and W.C. Walter (1969). Seismic Energy Sources. Houston, TX, Offshore Technology Conference. Paper OTC 1119, v. 2 Preprints, p. 387-416.

24. Krause, Dale C. (1962). Interpretation of Echo Sounding Profiles. Int. Hydrog. Rev., v. 39, p. 65-123.

25. Larner, K.L., E.J. Mateker, Jr., and C. Wu (1973). Amplitude: Its Information Content. Mexico City, Mexico, 43rd Annual International Meeting of the Society of Exploration Geophysicists. Preprint.

26. Leong, W.K., T.K. Kan, and C.S. Clay (1971). Use of Acoustic Scattering Theory to Interpret Marine Geophysical Data. University of Wisconsin, Madison. Univ. of Wisc. Res. Rpt., Series #71-1, 32 p.

27. Luehrmann, W.H., T.R. Shugart, and W.H. Parker (1970). Marine Seismic Streamer Noise Analyses and Tests. Presented at 40th Annual Meeting of the Society of Exploration Geophysicists (abs.).

28. MacClure, D.C., H.F. Nelson, and W.B. Huckabay (1958). Marine Sonoprobe System, New Tool for Geologic Mapping. Am. Assoc. Pet. Geol. Bull., p. 701-716.

29. Mero, Thomas and John Freitag (1974). Seismic Source Signature Analysis. U.S. Naval Oceanographic Office, Technical Note 6222-5-74, 29 p., (unpub.).

30. Musgrove, A.W. (1962). Application of the Expanding Reflection Spread. Geophysics, v. 27, p. 981-993.

31. National Defense Research Committee (1946). Principles and Applications of Underwater Sound. Washington, DC, Summary Technical Report of Division 6, v. 7, 295 p.

32. Olhovick, V.A. (1964). The Causes of Noise in Seismic Reflections and Refraction Work. Geophysics, v. 29, p. 1015-1030.

33. Padberg, L.R., Jr. (1958). Subsurex - A New Approach to Geophysical Exploration Using Sonic Frequencies. World Petrol., March, p. 60-63.

34. Ricker, N. (1953). Wavelet Contraction, Wavelet Expansion and the Control of Seismic Resolution. Geophysics, v. 18, p. 769-792.

35. Schoenberger, Michael (1970). Optimization and Implementation of Marine Seismic Arrays. Geophysics, v. 35, p. 1038-1053.

36. Schoenberger, M. and F.K. Levin (1974a). Apparent Attenuation Due to Intrabed Multiples. Geophysics, v. 39, p. 278-291.

37. Schoenberger, M. and J.F. Mifsud (1974b). Hydrophone Streamer Noise. Geophysics, v. 39, p.781-793.

38. Smith, Mark K. (1956). Noise Analysis and Multiple Seismometer Theory. Geophysics, v. 21, p. 337-360.

39. Smith, Mark K. (1958). A Review of Methods of Filtering Seismic Data. Geophysics, v. 23, p. 44-47.

40. Smith, W.O. (1958). Recent Underwater Surveys Using Low Frequency Sound to Locate Shallow Bedrock. Bull. Geol. Soc. Am., v. 69, p. 69-98.

41. Thompson, Jay F. (1963). A Technique for Solving the Low-Velocity Problem. Geophysics, v. 28, p. 869-876.

42. Tucker, P.M. and H.J. Yorston (1973). Pitfalls in Seismic Interpretation. Tulsa, OK, Society of Exploration Geophysicists, Monograph 2, 50 p.

43. Urick, R.J. (1967). Principles of Underwater Sound for Engineers. New York, McGraw-Hill, 342 p.

44. U.S. Naval Oceanographic Office (1966). Handbook of Oceanographic Tables. Washington, DC, U.S. Government Printing Office (SP-68), 427 p.

45. Widness, M.B. (1973). How Thin is a Thin Bed? Geophysics, v. 38, p. 1176-1180.

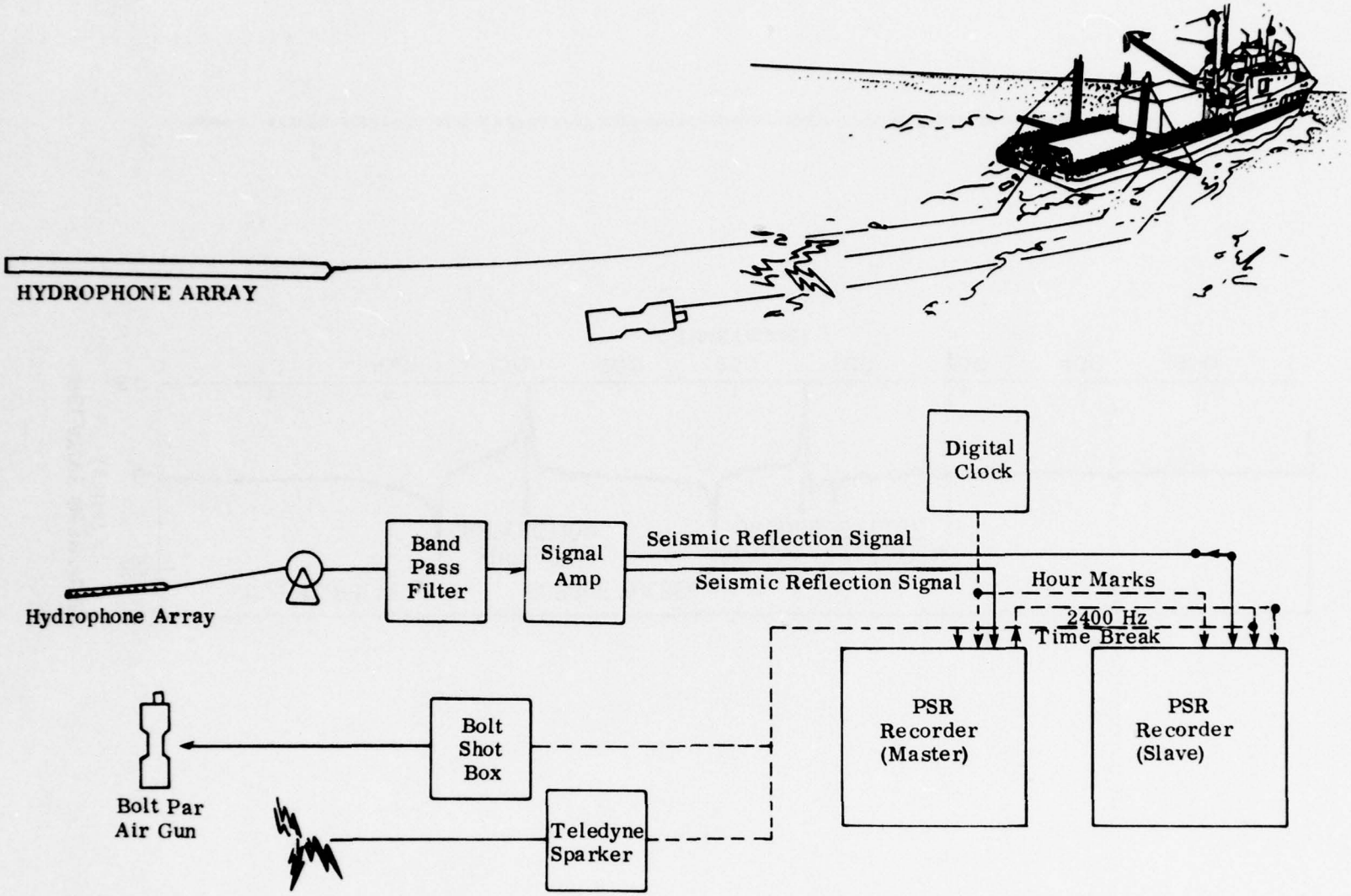

Figure 1. Sketch of a standard towing arrangement and block diagram of a typical single-channel shipboard seismic reflection configuration. In routine operations, a single sound source is used. The filter and amplifier are usually packaged in a single unit.

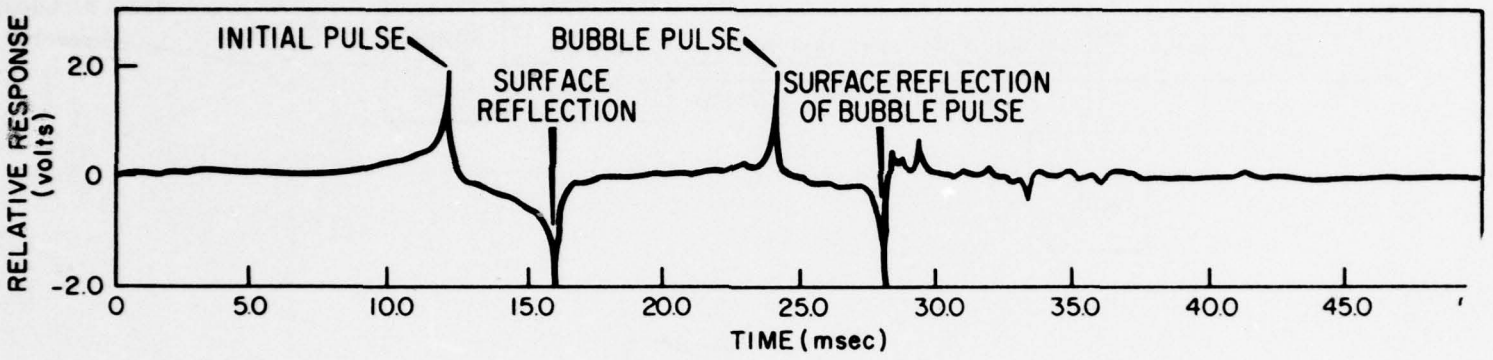

Figure 2. Broadband source signature of a 30-kJ, 15-kV single electrode sparker towed at 3.0m beneath the surface, after Mero and Freitag (1974)

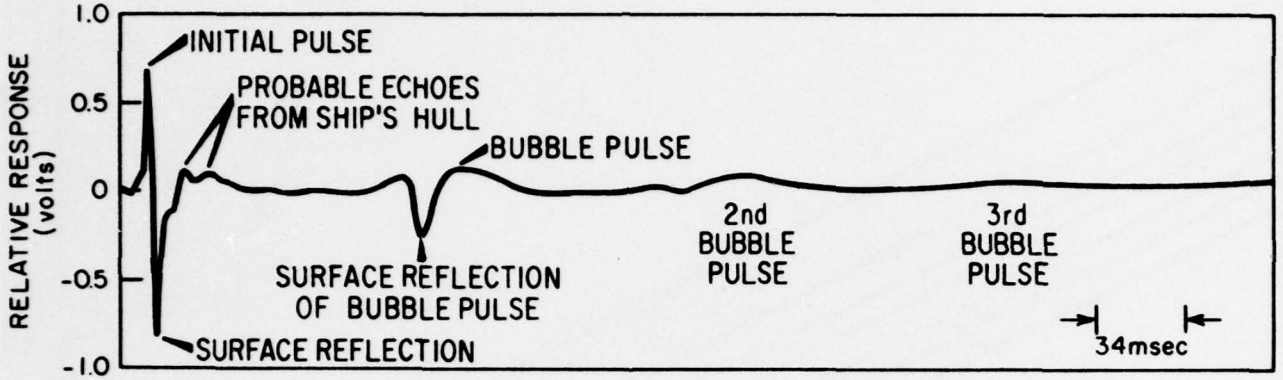

Figure 3. Broadband source signature of a 225-in^3 air gun charged to 2000 psi and suspended 4.6m below the surface. Note complication added by onset of surface reflection of bubble pulse before expansion of air bubble is completed. after Mero and Freitag (1974)

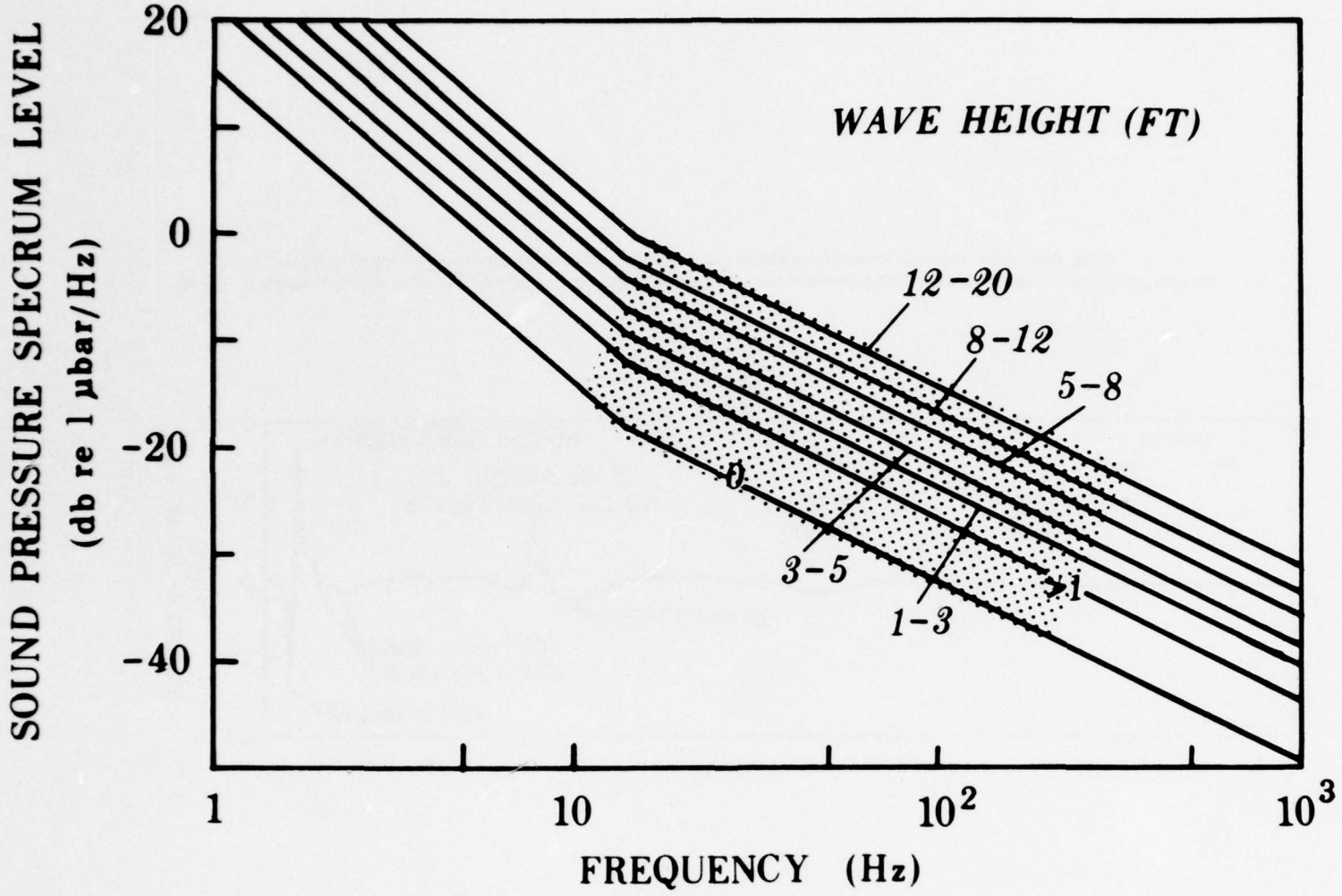

Figure 4. The frequency and intensity of noises generated by waves up to 20 feet high. At seismic frequencies, indicated by stippled zone, wave noises produced by a moderate sea may easily exceed signal levels. after Urick (1976)

Figure 5. Noise interference on a seismic record. The heavy dark bands near the center of the illustration are radio transmissions picked up by the hydrophone array lead-in cable and the gray areas on the right are passing ship traffic.

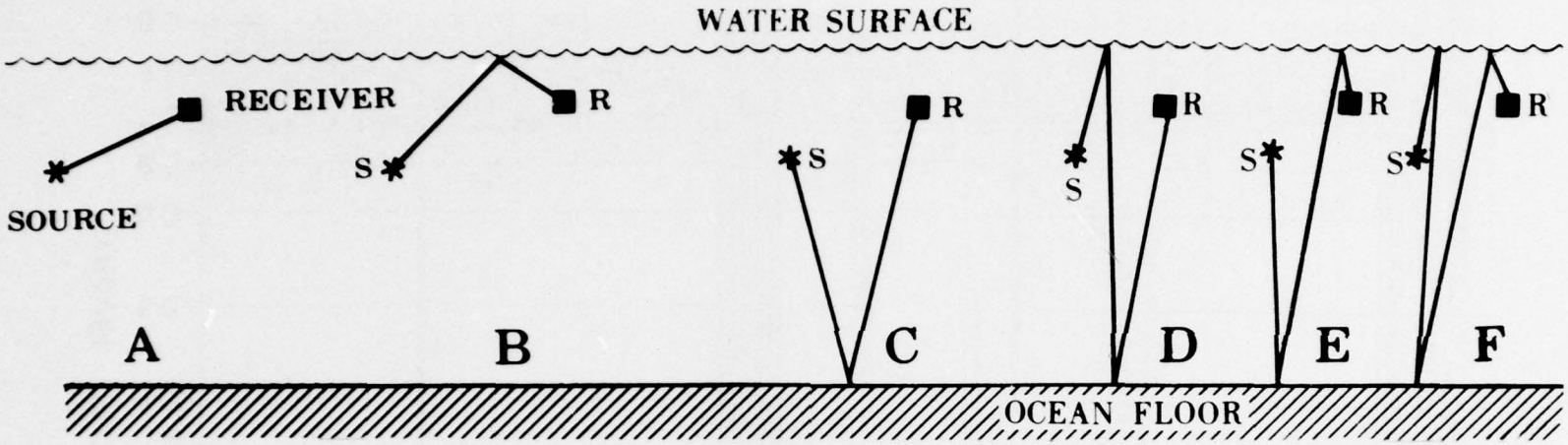

Figure 6. Paths followed by the primary sound ray between source and receiver. A and B are the first dark lines at the top of a record. C through F are rays forming the echo sequence from a single interface. The bubble pulse and other secondary sources generate similar sequences of signals which are recorded along with these echoes.

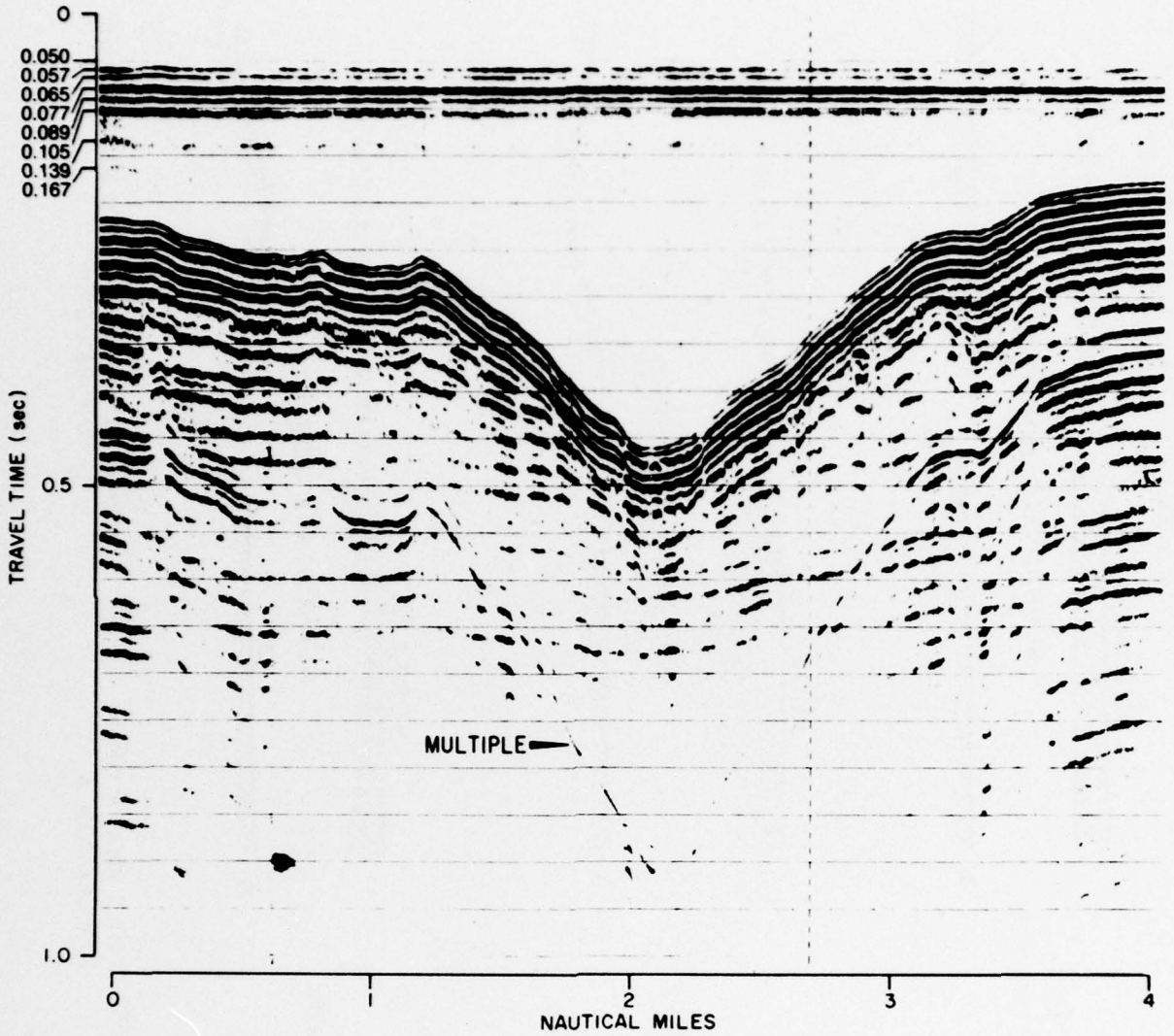

Figure 7. One-second firing rate, one-second sweep rate air gun record across Oceanographer Canyon. The 10-in^3 air gun was pressurized to 800 psi and towed about 1.5m below the surface. The recorded events between 0.057 seconds and 0.167 seconds are identified in the text.

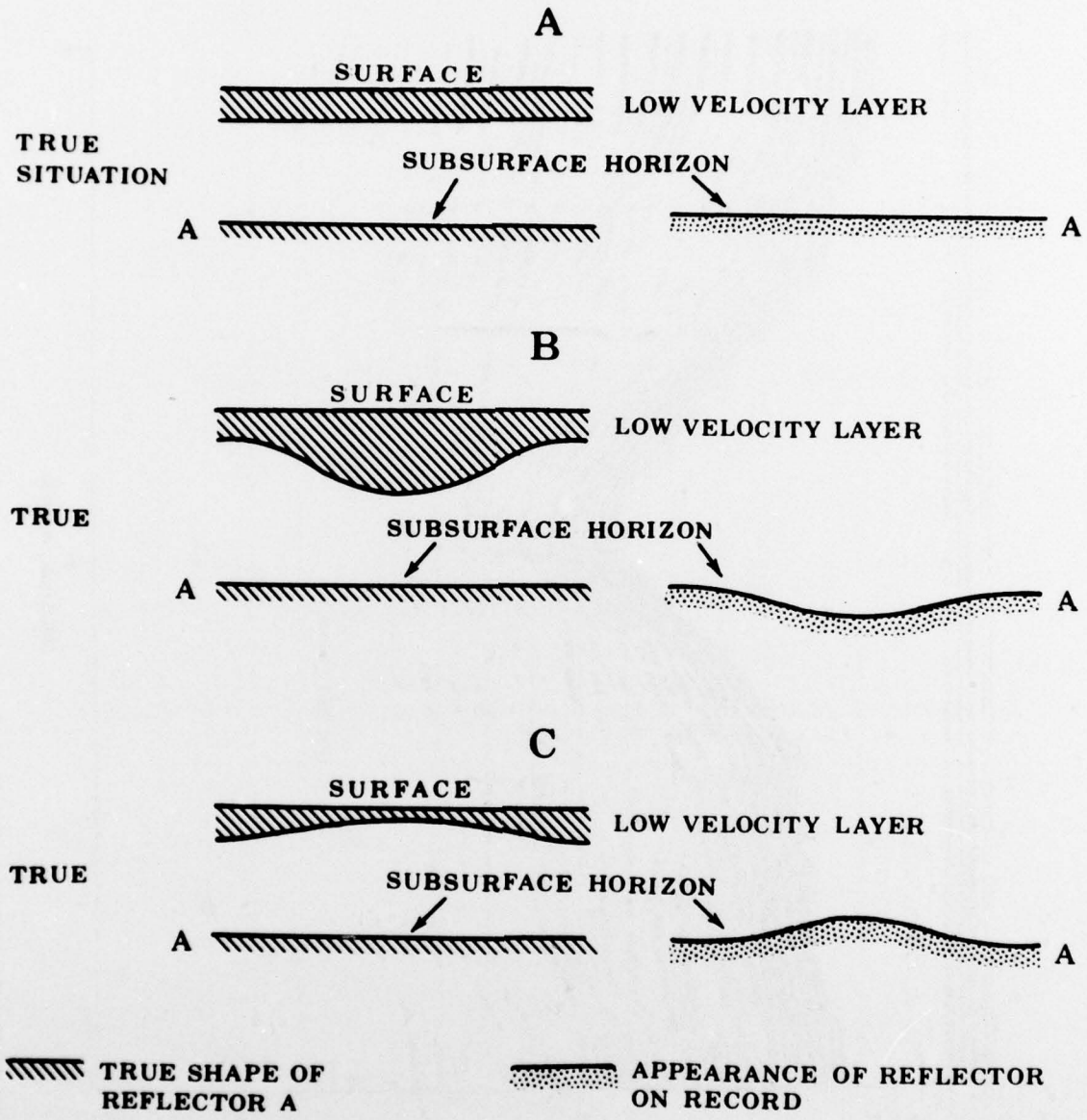

Figure 8. Effect of a low velocity layer on the recorded appearance of a horizontal reflector, after Thompson (196

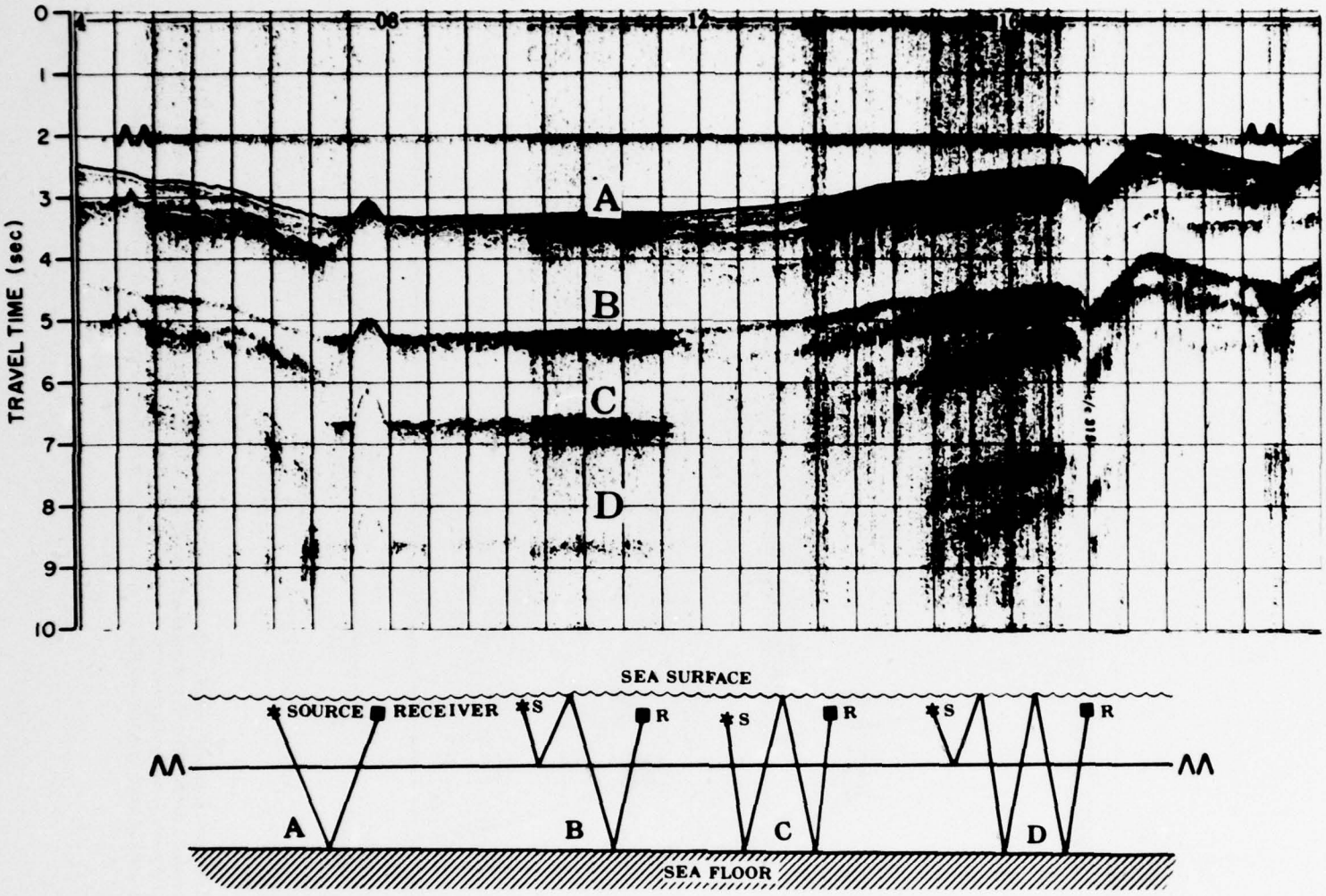

Figure 9. A multiple reflected event of unknown origin. Diagrams B and D are possibly ray paths for signals reflecting from the inhomogeneity at 2 seconds, while A and C are the bottom echo and its multiple.

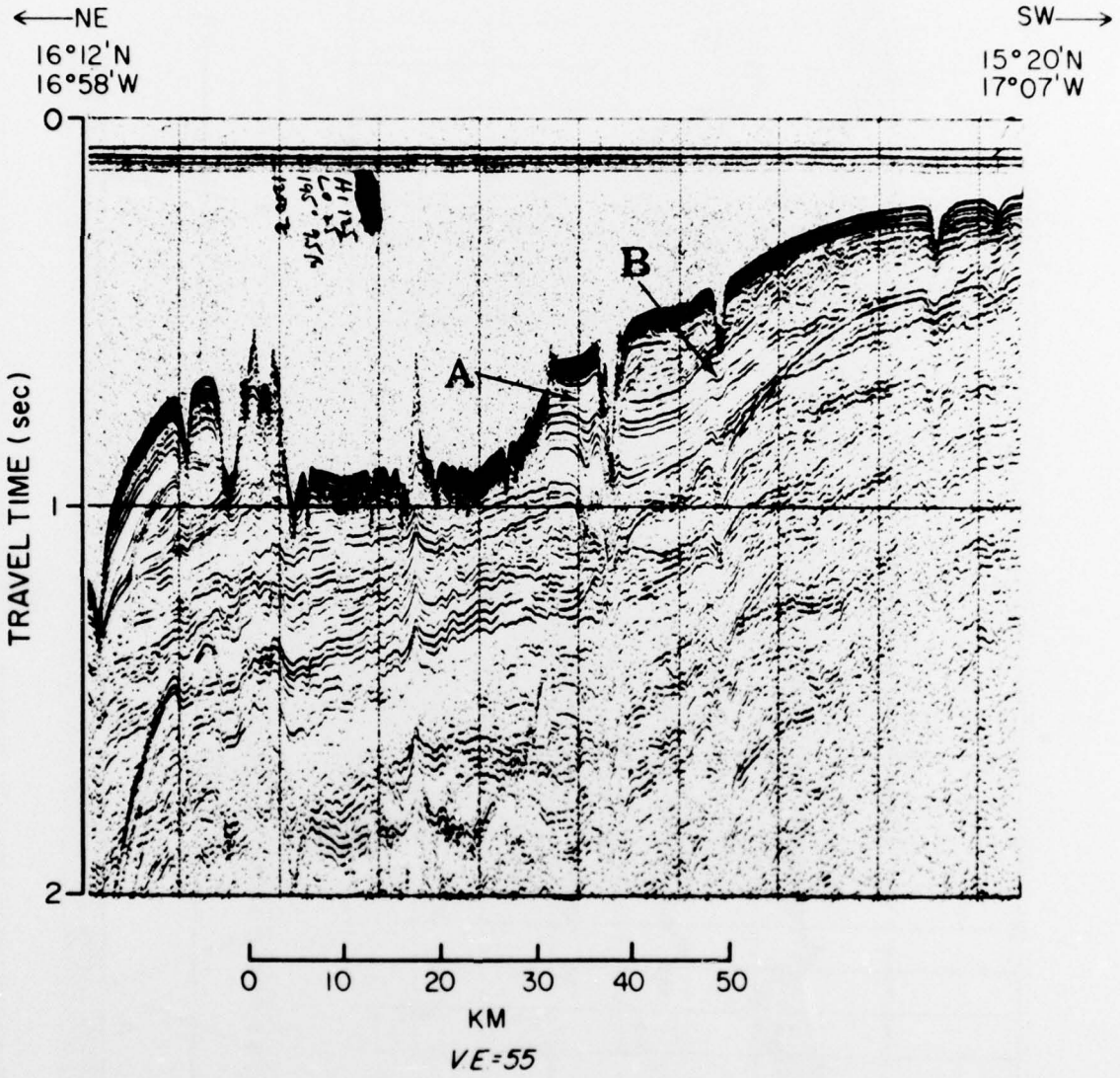

Figure 10. Synclines and erosional valleys along the Senegalese Continental Margin. Point A is an apparent syncline in which the dips of successively deeper reflectors increase with depth, possibly because of velocity increases with depth. Point B is an apparent syncline in which dips of successively deeper reflectors decrease and the entire structure widens with increasing depth. Point A in interpreted as a true syncline and Point B as an artifact of the increased thickness of an overlying low velocity layer (water, in this instance).

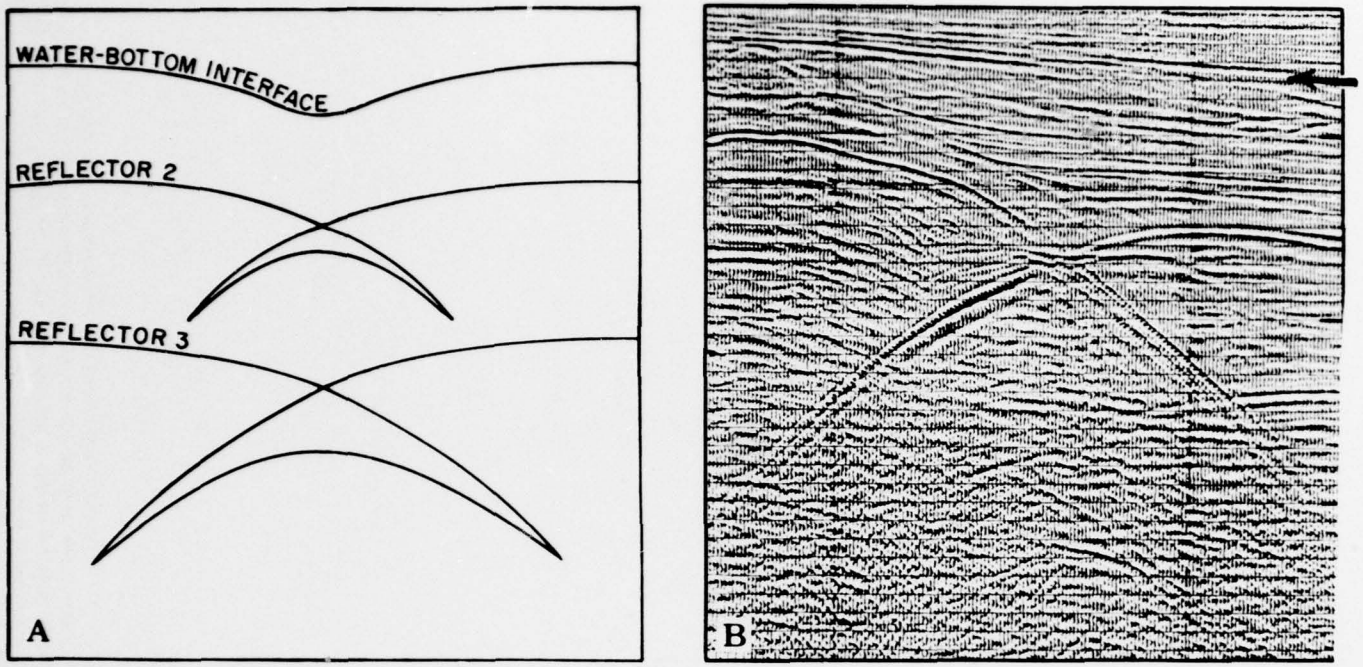

Figure 11. Sketch of an apparent anticline beneath a syncline. This pattern is caused by echoes from the sides of the syncline arriving aft reflection. The increase in width of the apparent anticline and the decrease in dip of the limbs with depth are clues to its true source. a and Yorston (1973)

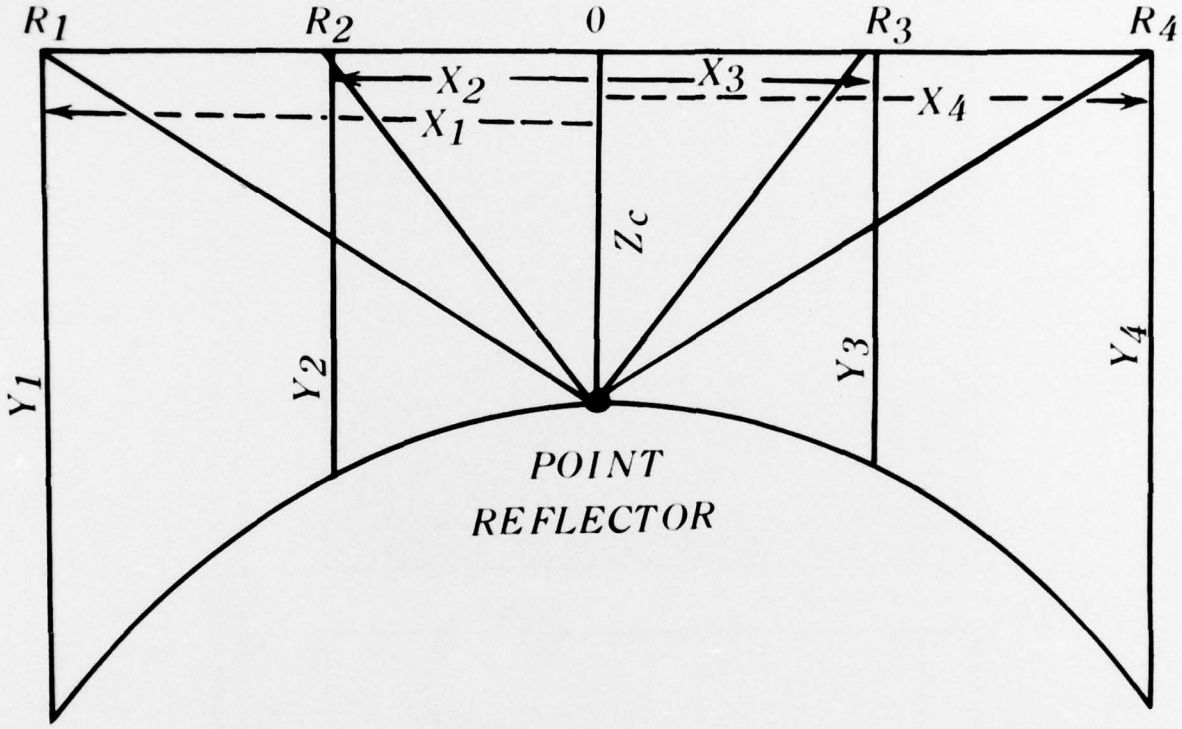

Figure 12. A sketch of Ball's technique for distinguishing diapirs from restricted area reflectors which generate apparent diapirs. R_1 through R_4 are receiver (ship) positions; z_c is water depth at the center of the structure; X_1 through X_4 are horizontal distances from the center of the structure; and Y_1 through Y_4 are water depths at receiver positions, as read from the record. If $(Z_c)^2 + (X_n)^2 = (Y_n)^2$, then the feature is very likely generated by a diffracted arrival. based on data from Ball (1969)

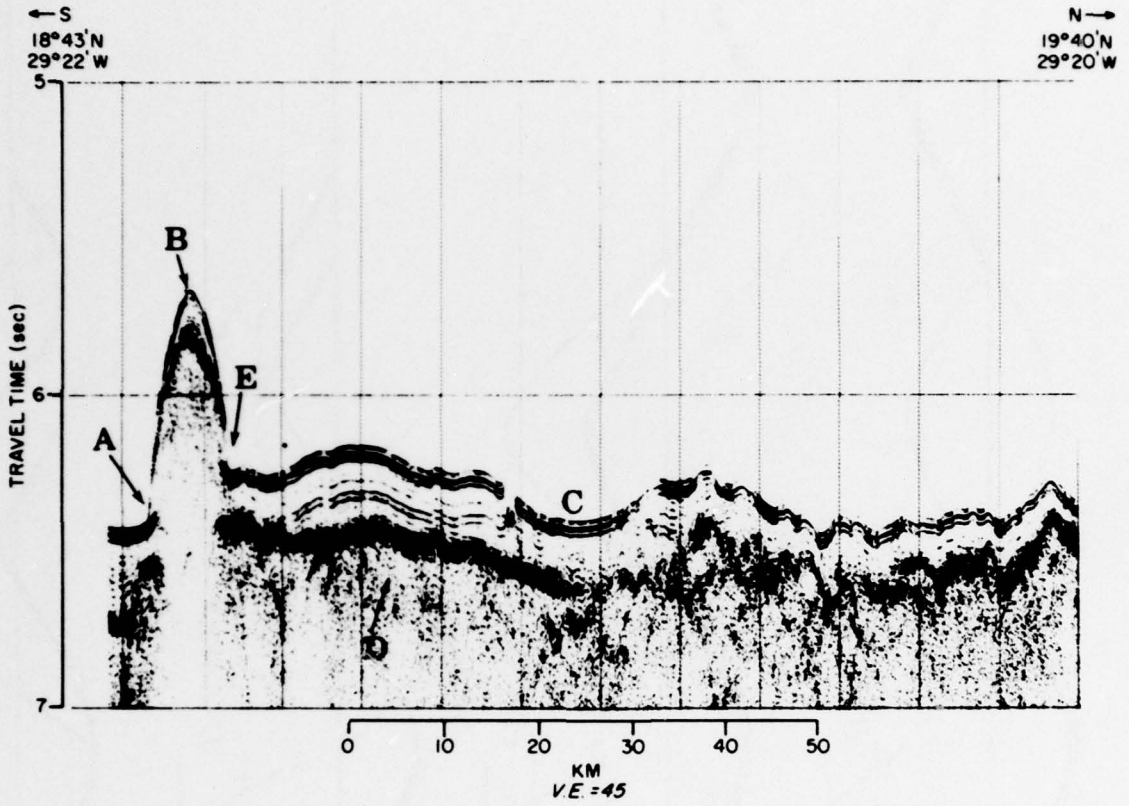

Figure 13. Record illustrating several reflection phenomena:

(A) Diffraction arriving ahead of true sea floor reflection;

(B) Amplitude decrease due to scattering (divergence) from a convex surface;

(C) Amplitude increase due to convergence on concave surface;

(D) Smooth basement with suggestion of layering. Reflections of this type may be produced by intrusions such as sills, lit sediments overlying true volcanic basement, or volcanic debris reworked by currents;

(E) Offset in sea floor caused by sediment ponding behind peak (B), or by faulting. Sediments are approximately the sar on opposite sides of the peak, therefore, faulting appears the more probable.

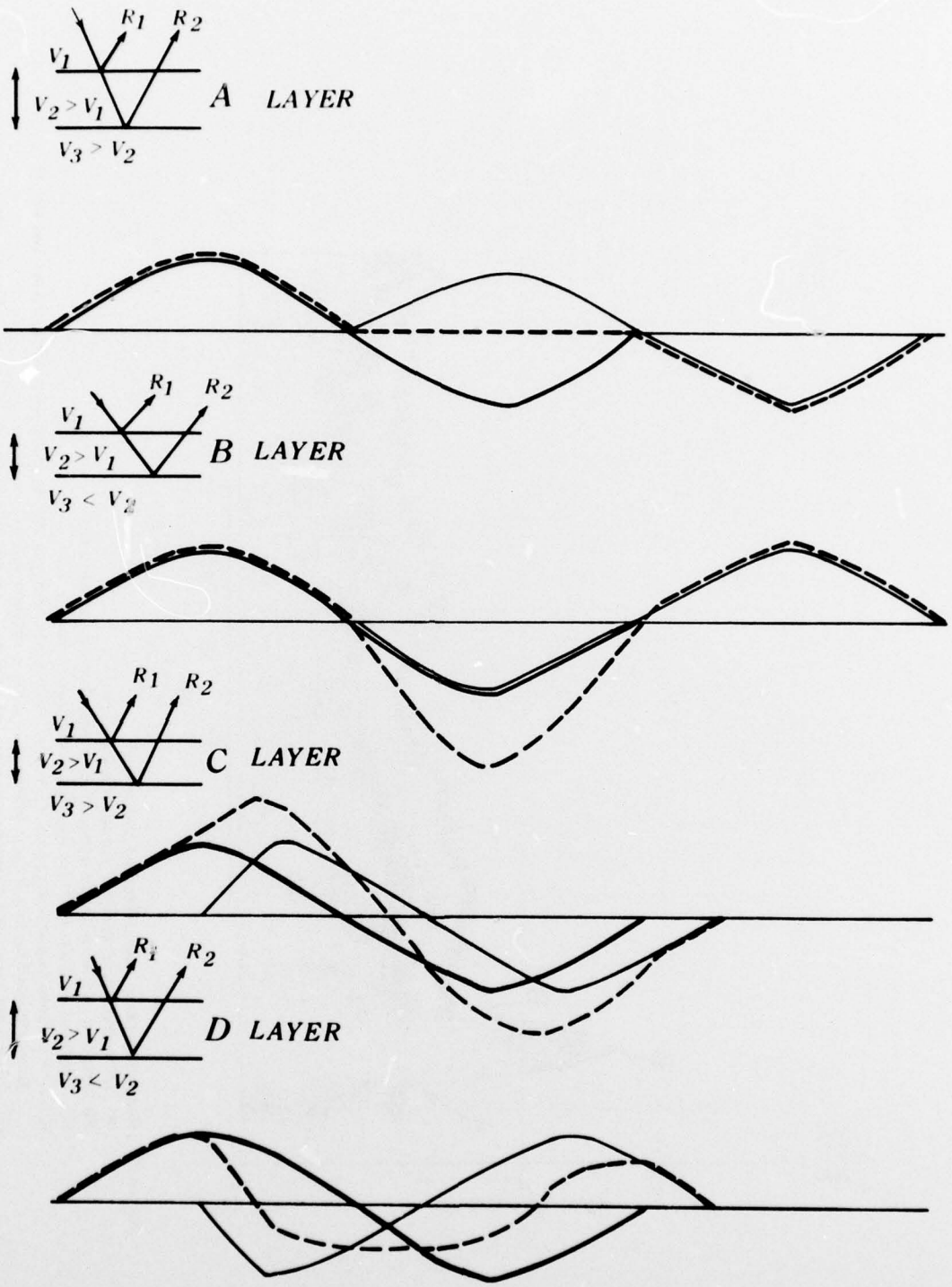

Figure 14. Schematic presentation of the recorded appearance of reflectors from layers with ½-wavelength separation (A and B), in which velocity increases with depth (A) and decreases with depth (B); (C and D) are representative of reflectors with ¼-wavelength separation when the velocity increases with depth (C) and decreases with depth (D). The dashed line represents the combined recorded intensity of the two individual signals (light and heavy lines).

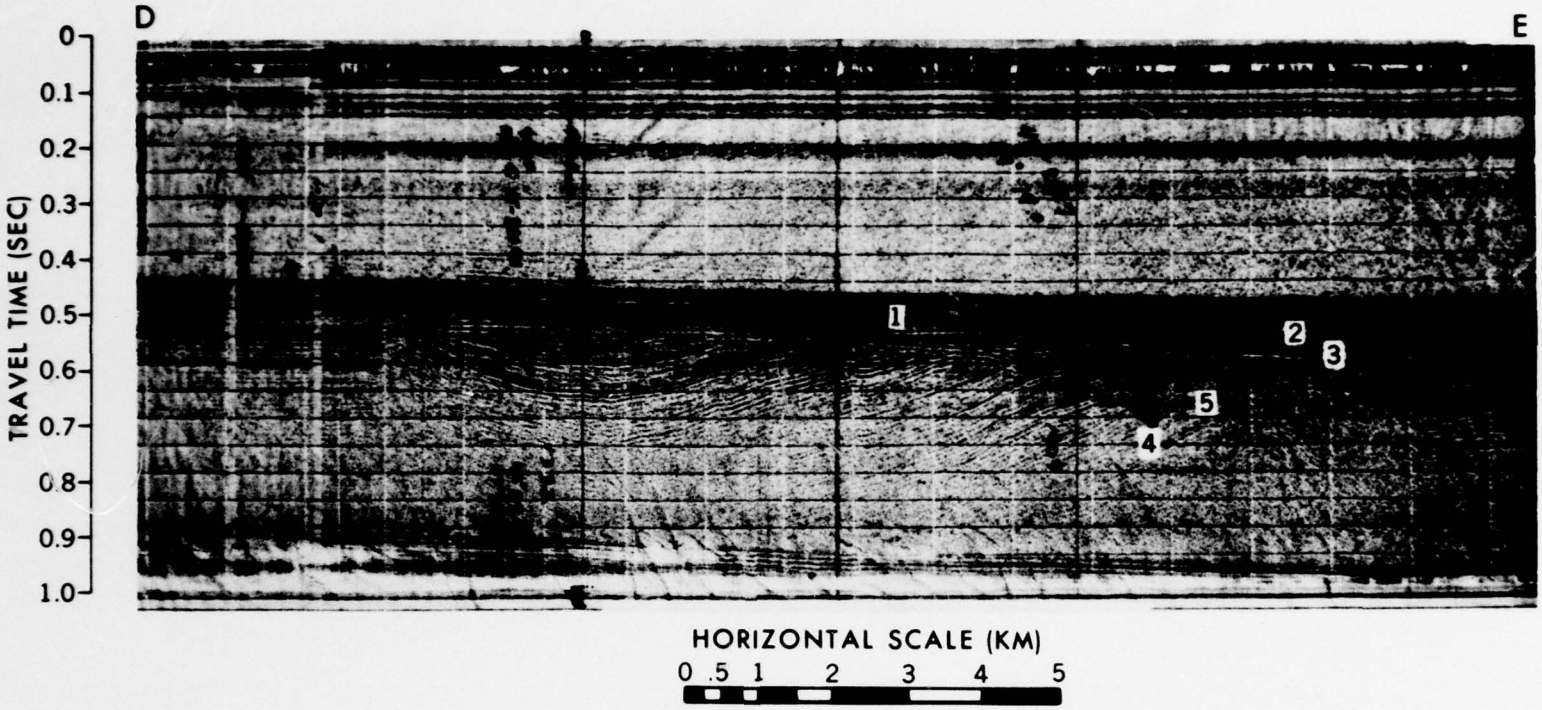

Figure 15. A geologic cross-section revealed by a seismic profile. Unit 5 is a folded, eroded sequence separated from unit 4 by an angular unconformity. Unit 4, a truncated channel fill deposit, is disconformable beneath highly reflective units 1 and 3, and nonstratified unit 2. after Ballard and Sorensen (1968)

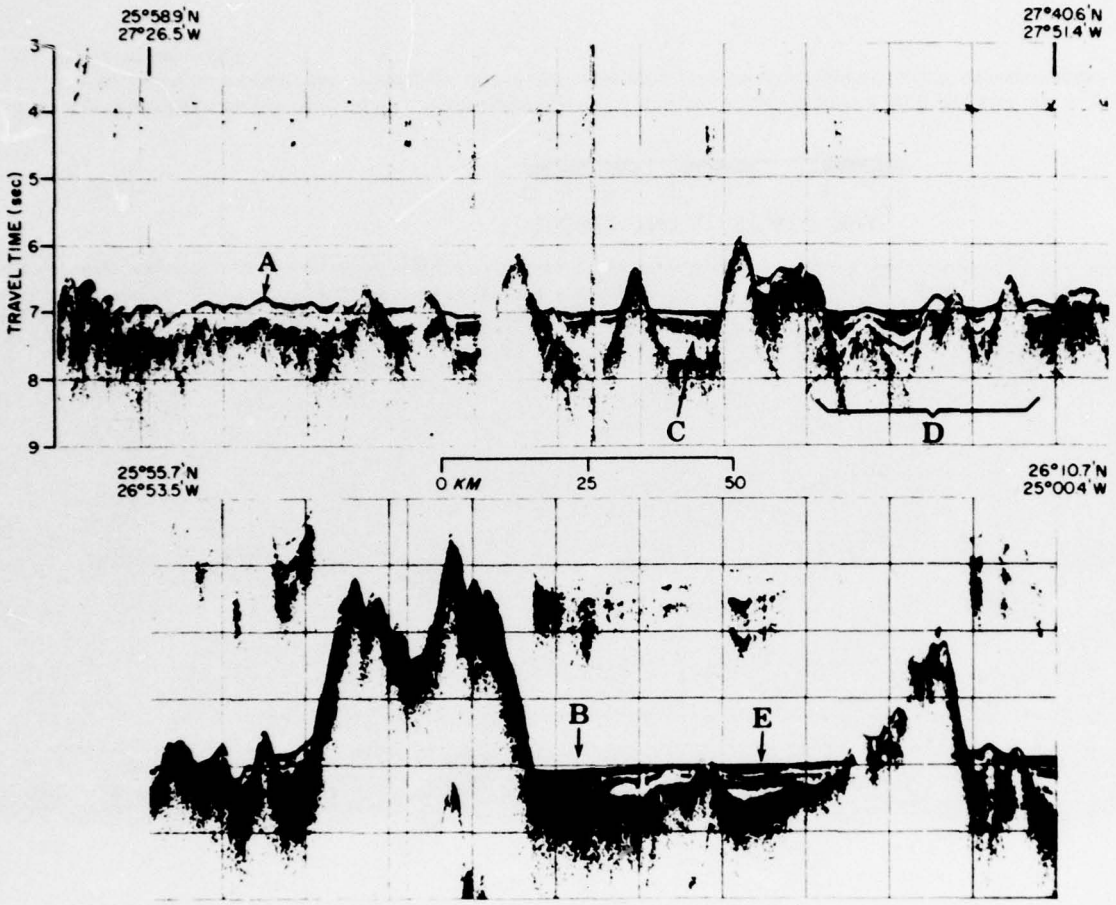

Figure 16. Typical Eastern North Atlantic Reflector Types:

(A) Upper acoustically transparent zone;

(B) Stratified zone, typical of turbidite deposits;

(C) Lower acoustically transparent zone;

(D) Typical "basement" in the Canary Basin;

(E) Location of Joides Drill site 138. Basement at this location has an acoustic signature different from that at (D).

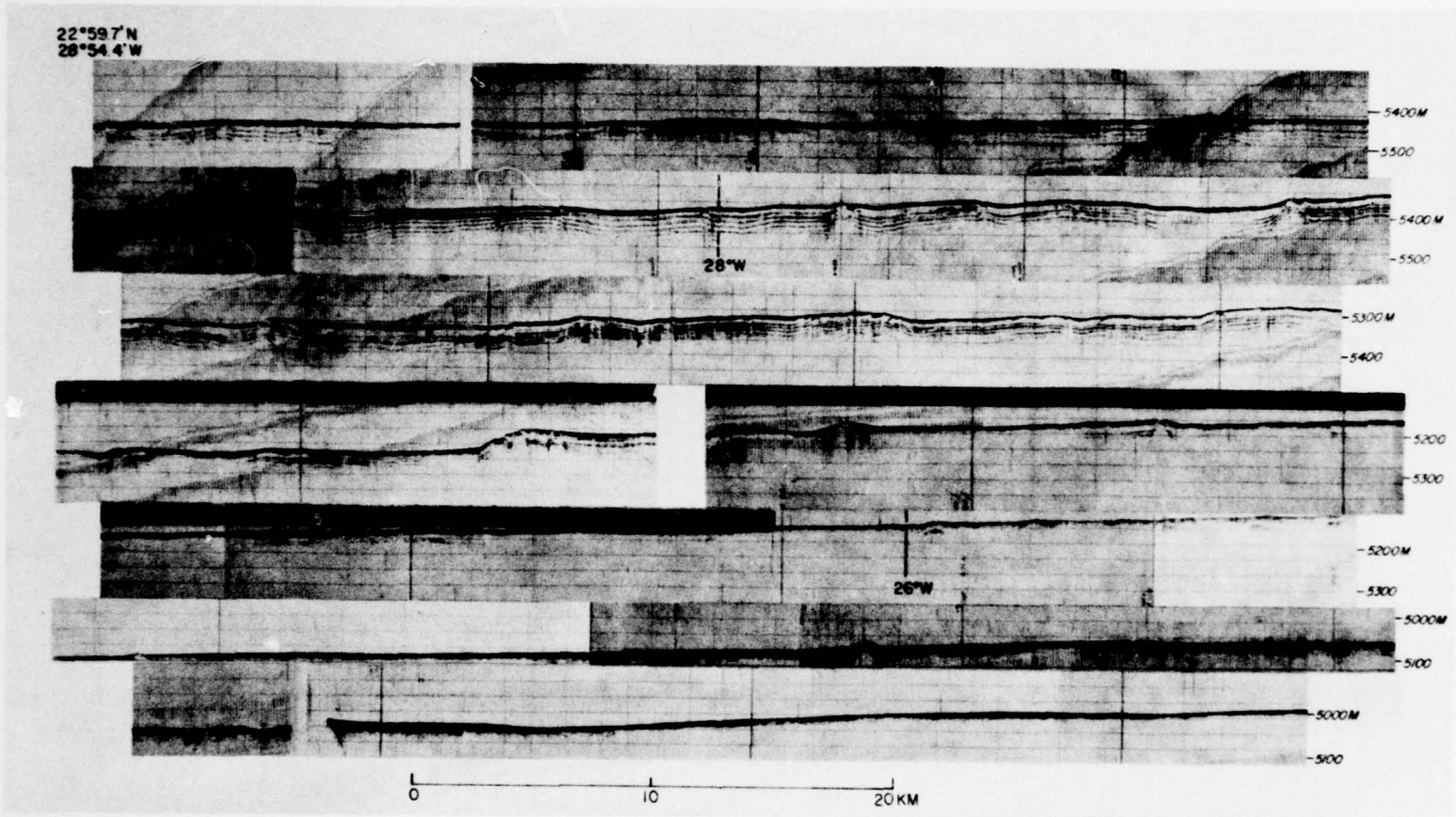

Figure 17. A 3.5 kHz record made along 23° N latitude between 29° W and 25° W longitude, (sections adjoin left to right, top to bottom.) Cross sections that appear smooth and acoustically transparent at seismic frequencies have numerous reflectors in the upper 50 m and some indication of creep and sediment ponding at higher frequencies and expanded scale.

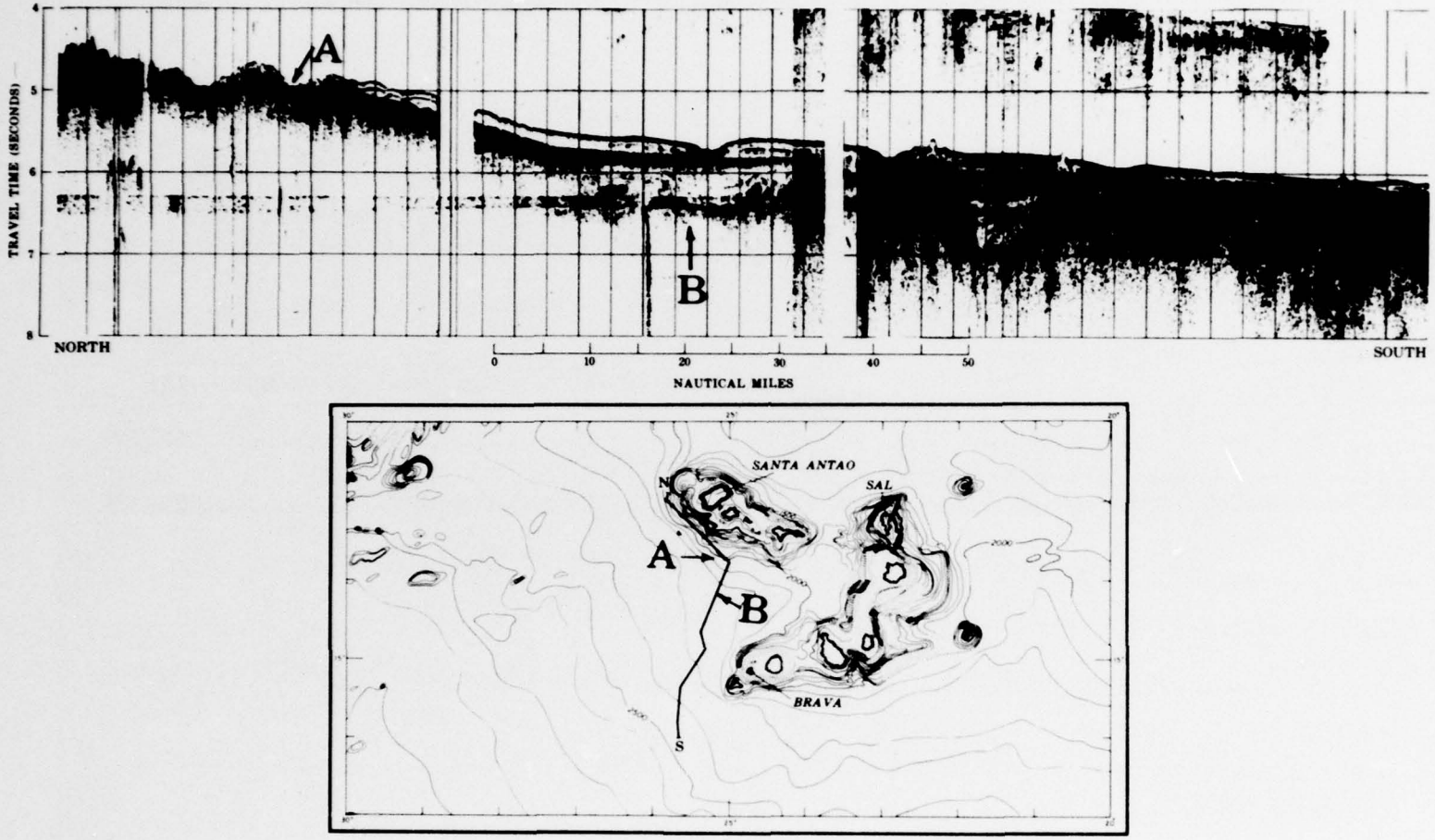

Figure 18. An example of "typical acoustic basement" (A), in which the echoes suggest a rough, highly reverberatory reflector. Down-slope "basement" changes to a layered or smoothly reflective "basement" beneath which another example of rough "basement" (B) can be seen, after Ballard and Hemler (1969)

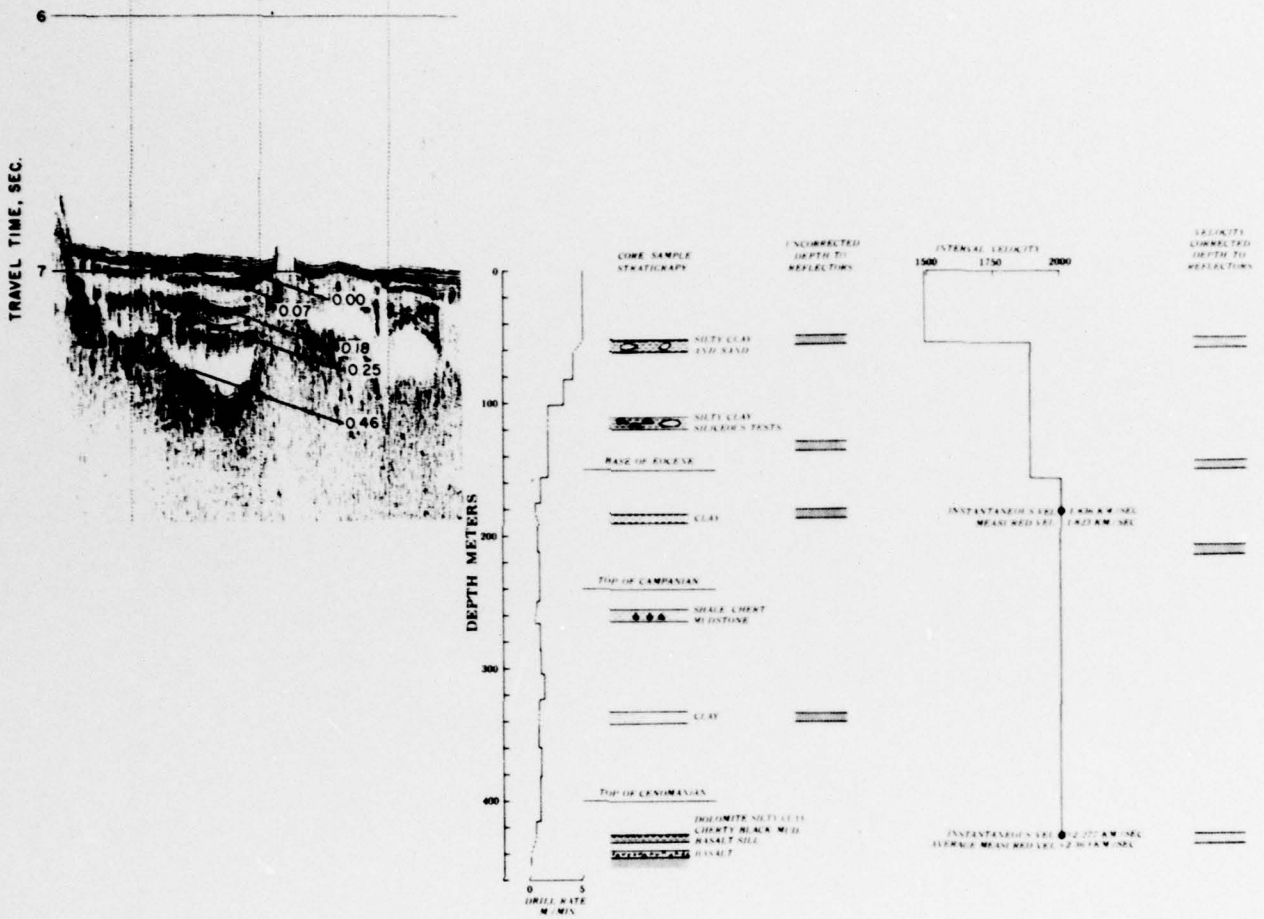

Figure 19. A comparison of a seismic record across Joides site 138 and data derived from drilling records. Measured velocities are those reported in the literature; instantaneous velocities are calculated using average interval velocity and an approximated initial velocity.

SECURITY CLASSIFICATION OF THIS PAGE (When Data Entered)

REPORT DOCUMENTATION PAGE		READ INSTRUCTIONS BEFORE COMPLETING FORM
1. REPORT NUMBER	2. GOVT ACCESSION NO.	3. RECIPIENT'S CATALOG NUMBER
4. TITLE (and Subtitle) Interpretation of Single-Channel Seismic Reflection Records		5. TYPE OF REPORT & PERIOD COVERED NORDA Report 1
		6. PERFORMING ORG. REPORT NUMBER
7. AUTHOR(s) J. Alan Ballard		8. CONTRACT OR GRANT NUMBER(s)
9. PERFORMING ORGANIZATION NAME AND ADDRESS Ocean Floor Division NOLI NORDA Bay St. Louis, Miss. 39520		10. PROGRAM ELEMENT, PROJECT, TASK AREA & WORK UNIT NUMBERS ~~133-81-612~~
11. CONTROLLING OFFICE NAME AND ADDRESS Naval Oceanographic Laboratory Naval Ocean Research & Development Activity Bay St. Louis, Miss. 39520		12. REPORT DATE FEB. 1977
		13. NUMBER OF PAGES 42
14. MONITORING AGENCY NAME & ADDRESS(if different from Controlling Office) N/A		15. SECURITY CLASS. (of this report) Unclassified
		15a. DECLASSIFICATION/DOWNGRADING SCHEDULE

16. DISTRIBUTION STATEMENT (of this Report)

Approved for public release; distribution unlimited

17. DISTRIBUTION STATEMENT (of the abstract entered in Block 20, if different from Report)

N/A

18. SUPPLEMENTARY NOTES

19. KEY WORDS (Continue on reverse side if necessary and identify by block number)

Seismic Reflection
Reflected Signal Identification
Velocity Correction
Seismic Source Level

20. ABSTRACT (Continue on reverse side if necessary and identify by block number)

The identification of signals recorded on a Single Channel Seismic reflection record is approached from instrumental environmental geometric and geologic viewpoints. Examples show that it is frequently possible to distinguish between noises, recorded instrumental artifacts, and acoustic impedence mixmatches indicative of geologically significant structural and sedimentological variations. Analog-to-digital conversion processes introduce little error into the data, but the failure to allow for vertical velocity gradients in the sedimentary column can lead to significant differences between true and apparent depths to reflectors. Failure to consider diffraction effects, vertical exaggeration effects, velocity effects and numerous other factors can lead to serious interpretation errors.

DD FORM 1 JAN 73 1473 EDITION OF 1 NOV 65 IS OBSOLETE
S/N 0102-014-6601

SECURITY CLASSIFICATION OF THIS PAGE (When Data Entered)